

## PUBLISHED VERSION

Marc E. H. Jones, Flora Gröning, Richard M. Aspden, Hugo Dutel, Alana Sharp, Mehran Moazen, Michael J. Fagan, Susan E. Evans

### **The biomechanical role of the chondrocranium and the material properties of cartilage**

Vertebrate Zoology, 2020; 70(4):699-715

© Senckenberg Gesellschaft für Naturforschung, 2020. This work is licensed under the Creative Commons Attribution License (CC BY 4.0)

<https://creativecommons.org/licenses/by/4.0/>

Published version <http://dx.doi.org/10.26049/VZ70-4-2020-10>

#### PERMISSIONS

<http://creativecommons.org/licenses/by/4.0/>



### Attribution 4.0 International (CC BY 4.0)

This is a human-readable summary of (and not a substitute for) the [license](#). [Disclaimer](#).

#### You are free to:

- Share** — copy and redistribute the material in any medium or format
- Adapt** — remix, transform, and build upon the material for any purpose, even commercially.

The licensor cannot revoke these freedoms as long as you follow the license terms.



#### Under the following terms:



**Attribution** — You must give [appropriate credit](#), provide a link to the license, and [indicate if changes were made](#). You may do so in any reasonable manner, but not in any way that suggests the licensor endorses you or your use.

**No additional restrictions** — You may not apply legal terms or [technological measures](#) that legally restrict others from doing anything the license permits.

24 March 2022

<http://hdl.handle.net/2440/134639>

# The biomechanical role of the chondrocranium and the material properties of cartilage

MARC E. H. JONES<sup>1</sup>, FLORA GRÖNING<sup>2</sup>, RICHARD M. ASPDEN<sup>2</sup>, HUGO DUTEL<sup>3,4</sup>, ALANA SHARP<sup>5</sup>, MEHRAN MOAZEN<sup>6</sup>, MICHAEL J. FAGAN<sup>4</sup> & SUSAN E. EVANS<sup>1</sup>

<sup>1</sup> Research Department of Cell and Developmental Biology, Anatomy Building, UCL, University College London, Gower Street, London, WC1E 6BT, UK; marc.jones@ucl.ac.uk — <sup>2</sup> School of Medicine, Medical Sciences and Nutrition, University of Aberdeen, Aberdeen, AB25 2ZD, UK — <sup>3</sup> School of Earth Sciences, University of Bristol, Bristol, BS8 1TQ, UK — <sup>4</sup> Department of Engineering and Computer Science, Medical and Biological Engineering Research Group, University of Hull, Hull, HU6 7RX, UK — <sup>5</sup> Institute of Life Course and Medical Sciences, University of Liverpool, Liverpool, UK — <sup>6</sup> Department of Mechanical Engineering, UCL, University College London, Torrington Place, London, WC1E 7JE, UK

Submitted September 14, 2020.

Accepted October 28, 2020.

Published online at [www.senckenberg.de/vertebrate-zoology](http://www.senckenberg.de/vertebrate-zoology) on November 24, 2020.

Published in print Q4/2020.

Editor in charge: Ingmar Werneburg

## Abstract

The chondrocranium is the cartilage component of the vertebrate braincase. Among jawed vertebrates it varies greatly in structure, mineralisation, and in the extent to which it is replaced by bone during development. In mammals, birds, and some bony fish, most of the chondrocranium is replaced by bone whereas in lizards, amphibians, and chondrichthyan fish it may remain a significant part of the braincase complex in adulthood. To what extent this variation relates to differences in skull biomechanics is poorly understood. However, there have been examinations of chondrocranium histology, *in vivo* strain, and impact on rostrum growth following partial removal of the chondrocranium. These studies have led to suggestions that the chondrocranium may provide structural support or serve to dampen external loads. Advances in computing-power have also facilitated an increase in the number of three-dimensional computer-based models. These models can be analysed (*in silico*) to test specific biomechanical hypotheses under specified loading conditions. However, representing the material properties of cartilage is still problematic because these properties differ according to the speed and direction of loading. The relationship between stress and strain is also non-linear. Nevertheless, analyses to date suggest that the chondrocranium does not provide a vertical support in lizards but it may serve to absorb some loads in humans. We anticipate that future models will include ever more detailed representations of the loading, anatomy, and material properties, in tandem with rigorous forms of model validation. However, comparison among a wider range of vertebrate subjects should also be pursued, in particular larvae, juveniles, and very small adult animals.

## Key words

Biomechanics; cartilage; chondrocranium; finite element analysis; *Salvator meriannae*; skull.

## Introduction

The chondrocranium is the cartilage portion of the vertebrate braincase (DE BEER, 1930, 1937; BELLAIRS & KAMAL, 1981; EVANS, 2008). It varies greatly among taxa with respect to its frame-like structure, mineralisation, as well as when and to what extent it is replaced by bone during ontogeny (DE BEER, 1930). There is also variation in how much of the chondrocranium, and associated endo-

chondral bone, contributes to the adult braincase (neurocranium) compared to the dermal roofing bones (COULY *et al.*, 1993). Variation in chondrocranium shape and development has been extensively documented since the 19<sup>th</sup> century (e.g., PARKER, 1883; GAUPP, 1900; HOWES & SWINNERTON, 1901; MEAD, 1909; DE BEER, 1930; PALUH & SHEIL, 2013; HAAS *et al.*, 2014). This work, coupled with

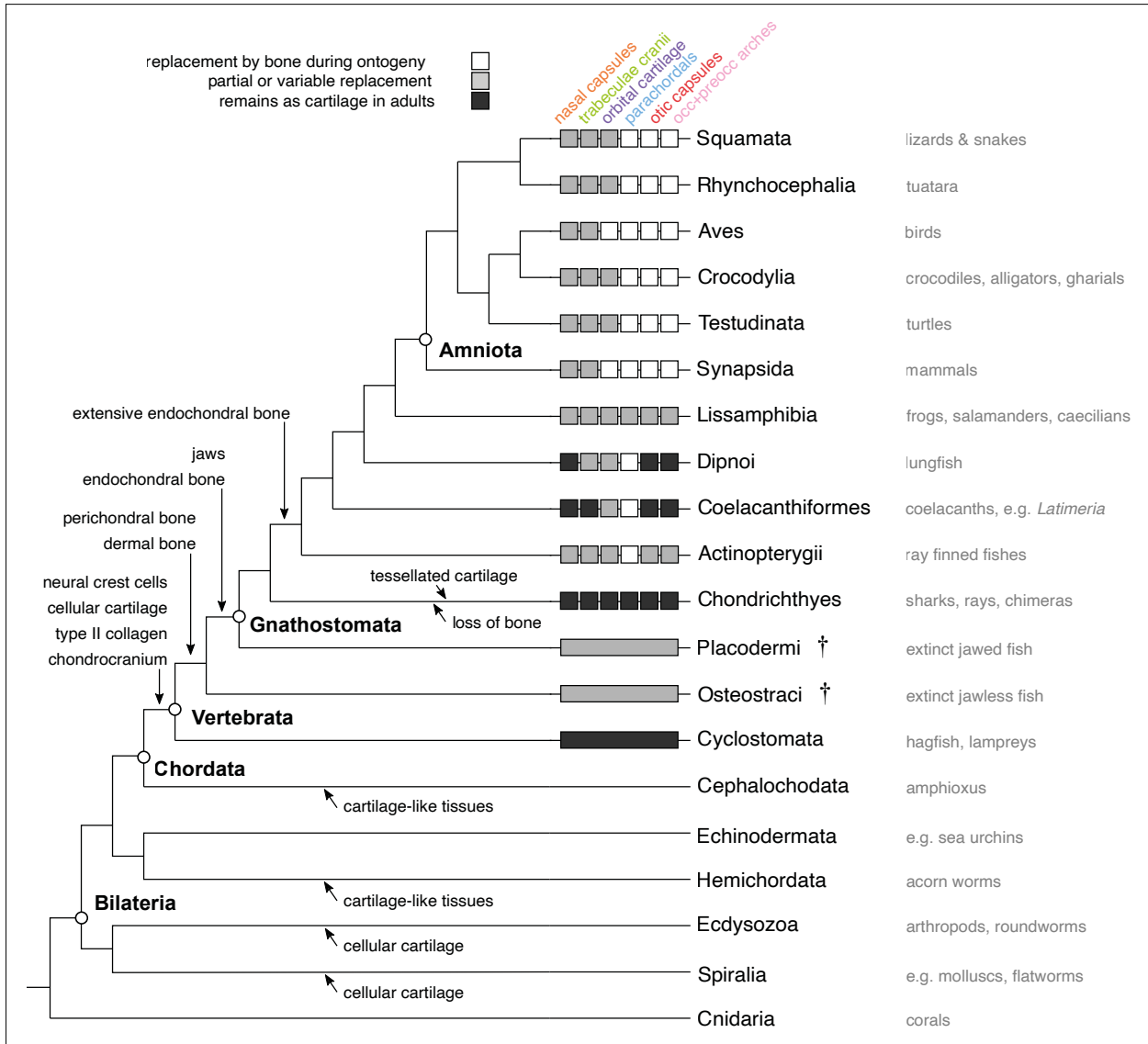


**Fig. 1.** A simplified phylogeny of Metazoa showing the general pattern of character distribution for cartilage, bone, and the chondrocranium (DE BEER, 1930; BELLAIRS & KAMAL, 1981; COLE & HALL, 2004a, b; DONOGHUE *et al.*, 2008; ZHU, 2014; ZHANG *et al.*, 2006; see also the excellent recent reviews KAUCKA & ADAMEYKO, 2019 and GILLIS, 2019). For each of the vertebrate groups, we have scored the six major components of the chondrocranium to reflect the extent of bone replacement during growth. These scores should be viewed as tentative and are admittedly crude and problematic for appreciating the full breadth of variation within clades. Dagger = extinct.

data from fossils (e.g., ATKINS *et al.*, 2009; ZHU, 2014), histology (e.g., COLE & HALL, 2004a, b), and molecular biology (e.g., ZHANG *et al.*, 2006; KAUCKA & ADAMEYKO, 2019; GILLIS, 2019), provides an understanding of chondrocranium character distribution, evolution, and disparity (Fig. 1).

The chondrocranium is a vertebrate character but the evolution of cartilage and its genetic regulatory network has a much deeper history within Bilateria (and possibly Metazoa) (COLE & HALL, 2004a, b; RYCHEL & SWALLA, 2007; COLE, 2011; KAUCKA & ADAMEYKO, 2019). Cartilage-like connective tissues are known to occur within Arthropoda, Mollusca, Brachiopoda, and Annelida where they often serve to protect the central nervous system and support the feeding apparatus (COLE & HALL, 2004a, b; RYCHEL *et al.*, 2007; KAUCKA & ADAMEYKO, 2019; GILLIS,

2019). Some of these tissues are cellular and histologically indistinguishable from the cartilage found in vertebrates (COLE & HALL, 2004a, b) and, in some taxa, they may even involve the same genes and signalling pathways (TARAZONA *et al.*, 2006). However, the patchy phylogenetic distribution of cellular cartilage is suggestive of multiple independent or parallel origins (COLE & HALL, 2004a, b; GILLIS, 2019). A cartilage-like tissue is present in cephalochordates where it supports the pharynx. However, this tissue lacks cells and does not form a framework to protect the sensory structures (RYCHEL & SWALLA, 2007; FISH, 2019).

The origin of the chondrocranium in vertebrates is linked to the origin of neural crest cells (DONOGHUE *et al.*, 2008; SQUARE *et al.*, 2020; but see ABITUA *et al.*, 2012) and the capacity to generate type II collagen (ZHANG

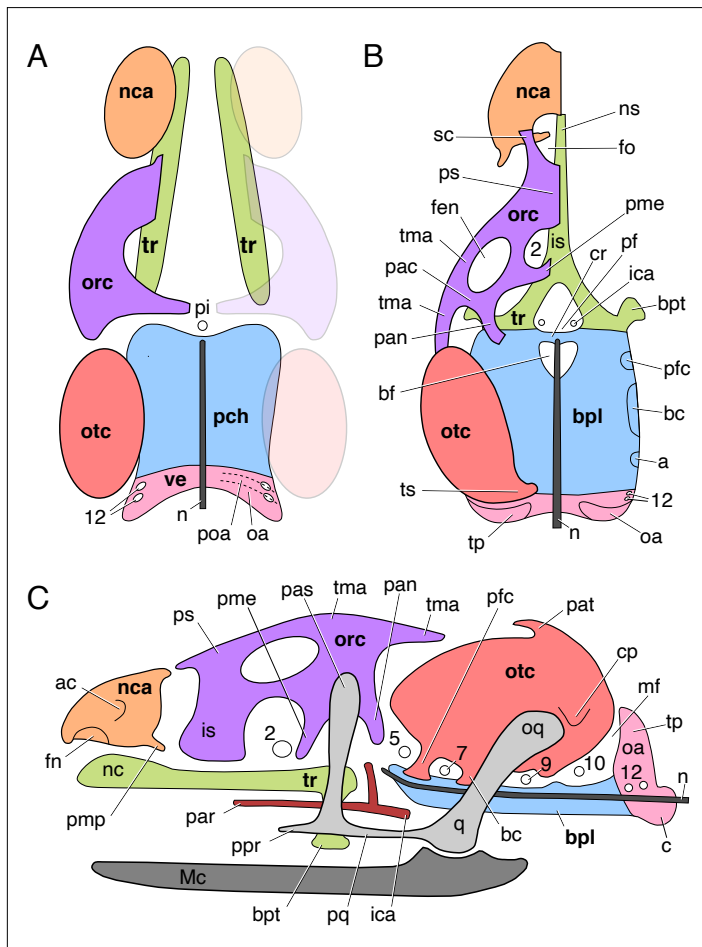


**Fig. 2.** A schematic diagram of a lizard-like chondrocranium (redrawn and modified from BELLAIRS & KAMAL, 1981). A, dorsal view of early stage showing the six main components of the chondrocranium: trabeculae cranii (tr), nasal cartilage of the ethmoid capsules (nca), otic capsule (otc), orbital cartilage (orc), parachordals (pch) fused to form the basal plate, and the vertebral elements (ve) which includes the occipital and preoccipital arches. The nasal cartilage, orbital cartilage, and otic capsule are transparent on the right side. B, dorsal view of later stage. The nasal cartilage, orbital cartilage, and otic capsule are absent on the right side. C, left lateral view of a later stage showing also parts of the mandibular arch and location of some cranial nerves. Note that some components are artificially separated. — *Abbreviations:* 2, optic nerve and fenestra; 5, trigeminal nerve roots in trigeminal notch (incisura prootica); 7, facial nerve; 9, glossopharyngeal nerve; 10, vagus nerve; 12, hypoglossal nerve foramina; a, region of apposition between otic capsule and basal plate; ac, aditus conchae; bc, basicapsular commissure; bf, basicranial fenestra; bpl, basal plate; bpt, basiptyergoid process; c, occipital condyle; cp, crista parotica; cr, crista sellaris; fn, fenestra narina; fen, fenestra epiotica; fo, fenestra olfactoria; ica, internal carotid artery; is, interorbital septum; Mc, Meckel’s cartilage; mf, metotic fissure; n, notochord; ns, nasal septum; oa, occipital arch; oq, otic process of the quadrate; pac, pila accesoria; pan, pila antotica; par, palatine artery; pas, ascending process of the pterygoquadrate (epipterygoid); pat, anterior process of tectum; pf, pituitary fenestra; pfc, prefacial commissure; pi, pituitary location; pme, pila metopica; pmp, posterior maxillary processes; poa, preoccipital arches; ppr, pterygoid process of the pterygoquadrate; pq, pterygoquadrate (intermediate part); ps, planum suprasetale; q, quadrate; sc, sphenethmoid commissure; tma, taenia marginalis; tp, tectum posterius; ts, tectum synoticum.

*et al.*, 2006). Hagfish and lampreys (Cyclostomata), as the only living jawless vertebrates, are important for understanding the evolution of the chondrocranium. However, they differ from one another and neither necessarily represents the ancestral condition (OISI *et al.*, 2013; KAUCKA & ADAMEYKO, 2019). They both possess an organised cartilage framework that provides structure to the sensory organs and support for the feeding apparatus (COURTOULD *et al.*, 2003; MARTIN *et al.*, 2009; OISI *et al.*, 2013; KAUCKA & ADAMEYKO, 2019), but it is difficult to find obvious shared homologies between parts from either framework in cyclostomes, and that of jawed vertebrates (gnathostomes) (OISI *et al.*, 2013). Fossils of extinct jawless fish, such as osteostracans, that lie on the stem of gnathostomes, exhibit armour-like plates of dermal bone and a braincase preserved in perichondral bone (JANVIER, 2008; KURATANI & AHLBERG, 2018).

Among gnathostomes, the chondrocranium has six recognisable components in development (Fig. 2A; DE BEER, 1937; BELLAIRS & KAMAL, 1981):

- 1.) the nasal capsules (which support the nasal apparatus and may form the ethmoid plate);
- 2.) the orbital cartilages (which are located medial to the eyes);
- 3.) the otic capsules (which contain the inner ear);
- 4.) the parachordals (which form the posterior base of the braincase);
- 5.) a pair of rod-like trabeculae cranii that sit between the parachordals and nasal capsules beneath the orbital cartilage and interorbital septum;
- 6.) the occipital and preoccipital arches (which enclose the posterior part of the brain).

The trabeculae cranii eventually meet in the midline anteriorly to form the internasal septum (BELLAIRS & KAMAL, 1981). The chondrocranium includes more conspicuous sheet-like components and provides more complete support of the neurosensory apparatus (KAUCKA & ADAMEYKO, 2019). Nevertheless, within gnathostomes there is considerable variation to the extent and timing of the replacement of the chondrocranium by bone.

In extant chondrichthyan fish (sharks, rays, and chimaeriforms), the chondrocranium provides the bulk of the skull including the dorsal roof of the braincase (MAISEY, 2013; MARA *et al.*, 2015; COATES *et al.*, 2017). The cartilage is not replaced by endochondral bone even in adults and dermal bone is entirely absent. However, the outer layer of chondrichthyan cartilage incorporates a shell of mineralised blocks or tesserae that provides stiffness (DEAN & SUM-

MER, 2006; MAISEY, 2013; PORTER *et al.*, 2013; LIU *et al.*, 2014). It may also have internal calcified struts (MAISEY, 2013). Fossil and molecular evidence indicates that this absence of bone was not the ancestral condition for Chondrichthyes (DONOGHUE *et al.*, 2006; ZHU *et al.*, 2013; ZHU, 2014; LONG *et al.*, 2015; GILLIS, 2019; BRAZEAU *et al.*, 2020). Among chondrichthyans there is significant variation in the shape of the chondrocranium as well as how it is connected to the upper and lower jaws (e.g., MIYAKE *et al.*, 1992; WALLER & BARANES, 1991; HUBER *et al.*, 2005; HOWARD *et al.*, 2013; MARA *et al.*, 2015). There is also variation in levels of mineralisation that is potentially related to differences in loading during biting (WALLER & BARANES, 1991; HUBER *et al.*, 2005).

Among (non-tetrapod) osteichthyan fishes, the chondrocranium may be extensively replaced by bone during ontogeny but in a variable sequence (NORMAN, 1926; PATTERSON, 1975; BASDEN *et al.*, 2000; MATTOX *et al.*, 2014; KUBICEK & CONWAY, 2015). There may also be variation in the location of gaps between the eventual endochondral elements (PATTERSON, 1975). The dermal roofing bones form the roof of the braincase. Within Actinopterygii (ray-finned fish) there is variation in the shape and ossification of the braincase. Among end members of the least nested lineages, such as *Amia* (Amiidae), the chondrocranium remains largely cartilaginous, with regions of endochondral ossification (e.g., otic and occipital regions) (ALLIS, 1897; GRANDE & BEMIS, 1998), whereas the chondrocranium of *Polypterus* (Polypteridae) is more extensively replaced by bone (ALLIS, 1922). Sturgeons (Acipenseridae) and paddlefish (Polyodontidae) have a braincase that is largely cartilaginous and lined by perichondral ossifications (HILTON *et al.*, 2011; WARTH *et al.*, 2017).

Sarcopterygia includes tetrapods and two living lineages of lobe-finned fishes: coelacanth and lungfishes. Ancestrally, the neurocranium of sarcopterygians was divided into two halves by an intracranial joint and was extensively ossified, so that the neurocranial anatomy is relatively well-known for different fossil lobe-finned fishes and early tetrapods (LU *et al.*, 2012, 2016; AHLBERG *et al.*, 1996; CLACK, 1998; DOWNS *et al.*, 2008; PARDO *et al.*, 2014). Living lobe-finned fishes, however, diverge from this ancestral condition and large parts of the chondrocranium remain cartilaginous. The evolution of coelacanth is marked by an extensive reduction and a fragmentation of the endochondral ossification centres, which are separated by large cartilaginous regions in *Latimeria* and in Mesozoic coelacanth (FOREY, 1998; DUTEL *et al.*, 2019). It has been proposed that the remaining ossification centres are located in regions of high loading in *Latimeria* (FOREY, 1998), but this hypothesis has yet to be tested. The skull of living lungfishes (three genera; *Neoceratodus*, *Lepidosiren* and *Protopterus*) is extensively modified with respect to that of fossil lobe-finned fishes, and the neurocranium of living genera consists largely of cartilage (CLEMENT & AHLBERG, 2014). Here as well, this condition is the result of a secondary reduction as Devonian lungfishes display a well-ossified lateral wall to their neurocranium.

In amphibians (frogs, salamanders, caecilians) the chondrocranium provides a crucial framework to the head in many larval forms and there is extensive variation in structure among groups (HILTON, 1950; SOKOL, 1981; HAAS *et al.*, 2006; ROČEK *et al.*, 2016; KRINGS *et al.*, 2017a, b; THESKA *et al.*, 2019). Differences in the timing of replacement by bone have been used to assess phylogenetic relationships (e.g., LARSON & DE SÁ, 1998) but these differences presumably also have some relationship to function. The tadpoles of frogs can be predatory and or burrow (e.g., CANDIOTI, 2007; HAAS *et al.*, 2014; KLINGER-STROBEL *et al.*, 2020). Phylogenetic studies involving fossil data suggest that the evolution of modern clades is associated with a reduction in braincase ossification (ATKINS *et al.*, 2019), e.g., loss of the basioccipital, loss of the basisphenoid and reduction of the sphenethmoid to a paired element.

Within amniotes a general chondrocranial structure is evident from which homologies can be inferred (Fig. 2BC; DE BEER, 1937; BELLAIRS & KAMAL, 1981; WITMER, 1995; WERNEBURG & YARYHIN, 2019) but there is variation in the shape and presence of interorbital components such as the taenia marginalis (tma), pila metoptica (pme), and pila antotica (pan) (DE BEER, 1937; PALUH & SHEIL, 2013; SHEIL & ZAHAREWICZ, 2014).

In lepidosaurs (snakes, lizards, and tuatara) a significant portion of the chondrocranium may be retained into adulthood (KAMAL & ABDEEN, 1972; BELLAIRS & KAMAL, 1981). Adult lizards generally possess the nasal capsules, a nasal septum (derived from the anterior ends of the trabeculae cranii), an interorbital septum and central framework of slender bars (derived from the orbital cartilage and posterior ends of the trabeculae cranii) (e.g., GAUPP, 1900; DE BEER, 1930; BELLAIRS & KAMAL, 1981; ZADA, 1981; HUGI *et al.*, 2010; HERNÁNDEZ-JAMES, 2012; YAYHIN & WERNEBURG, 2018). However, there is also significant variation among lizards with respect to shape and mineralisation (PEARSON, 1921; DE BEER, 1930, 1937; KAMAL & ABDEEN, 1972; BELLAIRS & KAMAL, 1981; ZADA, 1981; HUGI, 2010; HERNÁNDEZ-JAMES, *et al.*, 2012; YAYHIN & WERNEBURG, 2018): the pila metoptica of the orbital cartilage may be replaced with an orbitosphenoid bone (BELLAIRS & KAMAL, 1981; EVANS, 2008); the pila antotica may be replaced by a pleurosphenoid; the trabeculae cranii may be replaced by a septosphenoid; parts of the planum supraseptale may be replaced by ventral processes from the frontal bones; and a ventral portion of the interorbital septum may become supported by a dermal parasphenoid rostrum (= cultriform process, BELLAIRS & KAMAL, 1981; EVANS, 2008). Such variation is suggestive of a relationship to function, skull mechanics, and life style (DE BEER, 1937; BELLAIRS & KAMAL, 1982; JONES *et al.*, 2017; YAYHIN & WERNEBURG, 2018) given the location of the cartilage in relation to the kinetic cranial joints (e.g., mesokinesis, metakinesis) of some lizards (HALLERMANN, 1992; PAYNE *et al.*, 2011; MEZZASALMA *et al.*, 2014). Similarly, the structural relationship between the nasal cartilage, trabeculae cranii, and orbital cartilage are important to rhinokinesis in snakes (CUNDALL & SHARDO, 1995). AS

previously noted, it seems unlikely that kinesis could have evolved without associated evolution of the chondrocranial structure (BELLAIRS & KAMAL, 1982; CUNDALL & SHARDO, 1995).

In turtles there is significant variation in shape among clades and large parts of the orbital and nasal cartilages persist into adulthood (KURATANI, 1999; PALUH & SHEIL, 2013; SHEIL & ZAHAREWICZ, 2014). Compared with other amniotes, turtles are characterised by closure of the fenestra epiotica, expansion of the planum suprasetale, and reduction of the taenia medialis (PALUH & SHEIL, 2013; SHEIL & ZAHAREWICZ, 2014). Among crocodylians differences in chondrocranial structure have been recorded between species (e.g., WERNEBURG & YARYHIN, 2019; FERNANDEZ-BLANCO, 2019) and a nasal septum remains present in adulthood (KLENNER *et al.*, 2016). There is significant variation among birds but replacement by bone is generally early and extensive (ZAHER & ABU-TAIRA, 2013; HÜPPI *et al.*, 2019). The nasal capsule and associated conchae are one of the few regions that remain cartilaginous (BOURKE & WITMER, 2016). As in lepidosaurs, some variation in chondrocranium structure may be associated with cranial kinesis (ZAHER & ABU-TAIRA, 2013).

Replacement of the chondrocranium in mammals is generally extensive with often only the nasal cartilage remaining into adulthood (SÁNCHEZ-VILLAGRA & FORASIEPI, 2017; LAVERNIA *et al.*, 2019; MAIER, 2020; SMITH *et al.*, in press). However, the nasal cartilage shows significant variation in form (BRUINTJES *et al.*, 1998; HÜPPI *et al.*, 2018). Much of the variation of facial cartilages among mammals appears related to sensory systems, communication, thermoregulation, and respiration (BOYD, 1975; HILLENIUS, 1992; MEISAMI & BHATNAGAR, 1998; HÜPPI *et al.*, 2018; WROE *et al.*, 2018; MAIER, 2020) but what it means for regional and total skull biomechanics in these taxa remains largely unexplored. In a recent review of the chondrocranium, it was suggested that plasticity of facial cartilages has reached its peak in humans (e.g., KAUCKA & ADAMEYKO, 2019: p. 10), but the variation in shape and mineralisation exhibited by other mammals, particularly bats (e.g., GÖBBEL, 2000; CURTIS & SIMMONS, 2018) makes this suggestion seem potentially anthropocentric.

Despite the wide structural variation of the chondrocranium among vertebrates its biomechanical role remains poorly understood (JONES *et al.*, 2017). This lack of analysis restricts functional interpretations. A more accurate representation of soft tissue structures in biomechanical models is also crucial for a more complete understanding of vertebrate skull mechanics (e.g., ZHANG *et al.*, 2001; HU *et al.*, 2003; KUPCZIK *et al.*, 2007; MOAZEN *et al.*, 2009; GRÖNING *et al.*, 2011; CURTIS *et al.*, 2011a, b, 2013; MANUEL *et al.*, 2014; TSE *et al.*, 2015; JONES *et al.*, 2017; LIBBY *et al.*, 2017; MCCORMACK *et al.*, 2017; LIPPHAUS & WITZEL, 2020). Here we review previous studies of the biomechanical role of the chondrocranium and provide some suggestions for future research.

## Experimental removal of the nasal cartilage

There have been several studies investigating the impact of removing part of the nasal cartilage in mammals, e.g., in rabbits (WEXLER & SARNAT, 1965; SARNAT & WEXLER, 1966; SARNAT, 2008), rats (MOSS *et al.*, 1967; GANGE & JOHNSTON, 1974; COPRAY, 1986), and guinea pigs (STENSTRÖM & THILANDER, 1970). Some of these studies involved large sample sizes and different experimental combinations of removal of the nasal cartilage and surrounding structures (STENSTRÖM & THILANDER, 1970). Typically, the experimental animals were early juveniles. After a set period of time the experimental animals were measured against control animals. The results suggest that removal of the cartilage does not prevent snout (rostral) growth but growth is abnormal (KEMBLE, 1973; GANGE & JOHNSTON, 1974; CORPRAY, 1986). The nasal bones are often found to be ventrally displaced and this might lead to problematic malocclusion (STENSTRÖM & THILANDER, 1970). The rare absence of the nasal cartilage in young humans can similarly lead to abnormal growth, particularly of the maxilla (KEMBLE, 1973; but see BERGLAND & BORCHGREVINK, 1974). These observations have led to suggestions that the nasal septum is not necessary for growth to occur but is instead required for maintaining structural integrity of the rostrum during growth. Rather than a site of growth, the nasal septum may serve as an important vertical support strut (MOSS *et al.* 1968; STENSTRÖM & THILANDER, 1970; KEMBLE, 1973). Removal of the nasal septum in adult rabbits has no obvious effect indicating that the cartilage has no major structural role in adult animals (SARNAT, 2008). More recent research on mammalian models has provided more detailed evidence of how the nasal septum is related to mammalian skull growth (e.g., McBRATNEY-OWEN *et al.*, 2008; KAUCKA *et al.*, 2018). To what extent these experiments on small mammals can be used to make general inferences for other vertebrates is uncertain. Similar experiments on non-mammalian taxa could help to address this issue but as with all animal experiments there are ethical concerns to evaluate.

## Strain *in vivo*

Strain gauges can be used to measure the surface strain of an anatomical structure due to loading (e.g., BUCKLAND-WRIGHT, 1978; ROSS & HYLANDER, 1996; THOMASON *et al.*, 2001; ROSS & METZGER, 2004; MARKEY *et al.*, 2006; CUFF *et al.*, 2015). There has been at least one investigation of nasal cartilage using strain gauges (AL DAYEH *et al.*, 2009). It involved miniature pigs (*Sus scrofa*), which are model organisms for mammalian skull biomechanics and have contributed greatly to our understanding of chewing, sutures, and strain distribution (e.g., HERRING & TENG, 2000; RAFFERTY *et al.*, 2003). Experimental animals were anesthetized and strain gauges were applied to the septoethmoid junction and the nasofrontal suture, and electrodes were inserted into the jaw muscles (AL DAYEH *et al.*, 2009). After a period of recovery, the animals were



encouraged to eat and the electrodes were used to measure muscle activity (AL DAYEH *et al.*, 2009). The animals were then re-anesthetised and fitted with a third strain gauge along the anterior end of the nasal cartilage. Whilst the animals were still anesthetised, the jaw muscles were tetanized to stimulate contraction (AL DAYEH *et al.*, 2009). The *in vivo* strain measurements indicated that the septum was subject to loading. Relative timing suggested that this loading was due to occlusion rather than muscle contraction. However, compression was anteroposterior rather than dorsoventral. No evidence was found to support a vertical strut role for the septum. Instead, a role related to absorbing dynamic strains that arise from feeding was suggested (AL DAYEH *et al.*, 2009).

## Histology and Material Properties

The chondrocranium is composed of cartilage, which is a type of connective tissue that can be both tough and flexible. Generally, it comprises water, collagen, proteoglycans, and cartilage cells: chondrocytes (LITTLE, 2011). Among mammals, cartilage may be classified as hyaline, elastic, or fibrous (COLE & HALL, 2004a). Hyaline cartilage has a metachromatic matrix, rounded cells, and extracellular collagen. Elastic cartilage is similar but the protein elastin is present in the extracellular matrix. Fibrocartilage, has a higher fibrous content (COLE & HALL, 2004a; GILLIS, 2019). Further variation is found within fish related to the proportion of cellular to intercellular matrix as well as the precise content of the intercellular matrix (BENJAMIN, 1990; DEAN & SUMMER, 2006; WITTEN *et al.*, 2010). Among elasmobranch fishes, blocks of mineralisation connected by ligaments to form tessellated cartilage (PORTER *et al.*, 2013; LIU *et al.*, 2014).

The microstructure and mineralisation of cartilage is related to the loading to which it is subjected in life (CARTER & WONG, 2003; AL DAYEH & HERRING, 2014). Therefore, the microstructure of the chondrocranium in a particular taxon may provide indications of its mechanical role. The cartilage found in the tetrapod chondrocranium is generally hyaline cartilage (BENJAMIN, 1990; AL DAYEH & HERRING, 2014; GRIFFIN *et al.*, 2016a; KLENNER *et al.*, 2016). It is avascular and includes large quantities of type II collagen but its exact composition varies among taxa and anatomical location (COLE & HALL, 2004a, b; AL DAYEH & HERRING, 2014; XIA *et al.*, 2012). A histological examination of the nasal septum in crocodiles found that it is associated with an underlying cord of highly elastic tissues. This structure might resist tensile strains and stabilize the long-axis of the rostrum during feeding (KLENNER *et al.*, 2016). Similarly, regional differences in the pig septum appear to support its possible role in dampening stress from feeding loads (AL DAYEH & HERRING, 2014).

The material properties of the chondrocranium can be estimated from measurements on cartilage using, for example, nano-indentation (HOCH *et al.*, 1983; EBENSTEIN & PRUITT, 2006), drop loading (JEFFREY & ASPDEN,

2006), quasi-static loading (e.g., PORTER *et al.*, 2006), and tensile extension (RICHMON *et al.*, 2005). Reported values for Young's modulus (or stiffness) of cartilage range from 0.4 to 564 MPa (e.g., FLAM, 1974; PORTER *et al.*, 2006; EDELSTEN *et al.*, 2010; COLUMBO *et al.*, 2014; AL DAYEH & HERRING, 2014; GRIFFIN *et al.*, 2006a; PETERS *et al.*, 2017; CUTCLIFFE & DEFRATE, 2020). This variation arises primarily from the rate and direction of loading but is also related to the collagen content, degree of mineralisation, hydration, and specimen preparation (LANGELIER & BUSCHMANN, 2003; GUPTA *et al.*, 2009; PETERS *et al.*, 2017; CHANG *et al.*, 2020). The structure of cartilage means it is stronger and stiffer in compression than in tension (CARTER & WONG, 2003). The response to compressive loading is governed largely by deformation of the highly hydrated matrix causing water to be squeezed out, the anionic charges on proteoglycans being brought closer together and stress-transfer to the tensile reinforcing collagen fibrils (WRIGHT & DOWSON, 1976; LITTLE *et al.*, 2011). The response is non-linear and depends strongly on the rate of loading. Some samples may appear stronger in tension if they have a surrounding layer of perichondrium (WESTREICH *et al.*, 2007); the perichondrium itself may bear some of the load or it may constrain the deformation of the cartilage thus apparently increasing the modulus by restricting Poisson's ratio effects (ASPDEN, 1990). Cartilage may be considered as a biological fibre-composite material in which the collagen fibres provide tensile reinforcement to a weak, highly-hydrated proteoglycan gel (HUKINS & ASPDEN, 1985; ASPDEN, 1994). The anisotropic material properties of cartilage are due to the anisotropic arrangements of the constituent collagen and proteoglycans (ASPDEN, 1994; XIA *et al.*, 2012; AL DAYEH & HERRING, 2014; KLENNER *et al.*, 2016). Studies have examined the relationship between histology and tensile failure for articular cartilage (e.g., SASAZAKI *et al.*, 2006) and found that the collagen fibres are able to reorientate relative to tensile strains.

Most analyses of cartilage have focused on mammalian articular cartilage (unmineralised hyaline cartilage) to better understand the biomechanics of postcranial joints (e.g., HOCH *et al.*, 1983; CARTER & WONG, 2003; FERGUSON *et al.*, 2003; LANGELIER & BUSCHMANN, 2003; BURGIN, 2003; MANSOUR, 2004; SASAZAKI *et al.*, 2006; EDELSTEN *et al.*, 2010; LITTLE *et al.*, 2011; BURGIN *et al.*, 2014). Due to the interstitial fluid flow within cartilage the modulus is strongly time-dependent and studies using impact loading provide Young's modulus values of 50 to 200 MPa (JEFFREY & ASPDEN, 2006; BURGIN *et al.*, 2014), whereas those using slow loading report values that are typically below 10 MPa (e.g., HOCH *et al.*, 1983; JIN & LEWIS, 2004; PETERS *et al.*, 2017).

Values for other types of vertebrate cartilage are available such as nasal, septal, and alar cartilages (e.g., ZAHNERT *et al.*, 2000; HU *et al.*, 2003; PORTER *et al.*, 2006; GUPTA *et al.*, 2009; AL DAYEH & HERRING, 2014; GRIFFIN, 2016a, b). These tissues have values that are less than 35 MPa and frequently less than 5 MPa (WESTREICH *et al.*, 2007; AL DAYEH & HERRING, 2014; COLUMBO *et al.*, 2013;

Griffin *et al.*, 2006a; Chang *et al.*, 2020). Some regional differences may exist (Griffin *et al.*, 2006a) as well as differences relating to the direction of loading (Richmon *et al.*, 2006). In pigs, the anterior nasal septum was found to have a higher compressive stiffness and lower tensile stiffness than the posterior portion (Al Dayeh & Herring, 2014: about 5 vs. 3 MPa and 0.5 vs. 0.8 MPa). Stiffness values are also available for human auricular cartilage (Zahnert *et al.*, 2000; Westreich *et al.*, 2007; Griffin *et al.*, 2016b). Again, there are some regional differences but stiffness is generally less than 3 MPa (Griffin *et al.*, 2016b) and rarely as high as 25 MPa (Westreich *et al.*, 2007). The higher values are likely related to a surrounding layer of perichondrium (Westreich *et al.*, 2007).

Mineralisation adds stiffness to cartilage such that quasi-static loading of mineralised cartilage (elasmobranch vertebrae) has Young's modulus values as high as 564 MPa (Porter *et al.*, 2006). The Young's modulus of the chondrocranium of chondrichthyan fish (tessellated cartilage) varies significantly between taxa (Porter *et al.*, 2013). In some species it may still be less than 50 MPa but in others it may exceed 700 MPa, or even in some regions, and under certain loading conditions, begin to approach the stiffness of bone (Porter *et al.*, 2013; Liu *et al.*, 2014; Wroe *et al.*, 2008).

## Biomechanical modelling

Finite element analysis (FEA) of virtual computer models of the skull provides a powerful tool for testing specific biomechanical hypotheses (e.g., Moazen *et al.*, 2008, 2009; Curtis *et al.*, 2011a, b; Marcé-Nogué *et al.*, 2015). The approach can involve many steps (Fig. 3). In brief, it involves building a model of the anatomical structure, subdividing it into many simpler elements, and specifying material properties, constraints and loads appropriate for the question of interest (Fagan, 1996; Dar *et al.*, 2002; Ross, 2005; Richmond *et al.*, 2005; Curtis, 2011; Rayfield, 2007; Tse *et al.*, 2015; Wilken *et al.*, 2020). The model output has to be compared to other sources of data to “validate” the results (e.g., Bright & Gröning, 2011).

### Anatomical model

In the past, representing the complex three-dimensional shape of the chondrocranium presented a significant challenge (Wood *et al.*, 1991; Lozanoff, *et al.*, 1993; Hofstadler-Deiques *et al.*, 2005): the chondrocranium can be small and delicate, and it lies deep within the skull. However, particularly in the last few years, a wealth of detailed computer models have been successfully built for a range of vertebrate taxa including the hagfish (*Eptatretus burgeri*; Oisi *et al.*, 2015), lamprey (*Lethenteron reissneri*; Oisi *et al.*, 2015), various sharks (Wroe *et al.*, 2008; Howard *et al.*, 2013; Mara *et al.*, 2015; McQuiston, *et al.*, 2017), coelacanth (*Latimeria*; Dutel *et al.*, 2019), various frogs (Roček *et al.*, 2016;

Krings *et al.*, 2017a, b), tuatara (*Sphenodon punctatus*; Yaryhin & Werneburg, 2019), turkey (*Meleagris gallopavo*; Bourke & Witmer, 2016), mouse (Kaucka *et al.*, 2018; Tesařová *et al.*, 2019), and various primates including humans (Lozanoff, *et al.*, 1993; Manuel *et al.*, 2014; Tse *et al.*, 2015; Leary *et al.*, 2015; Shamoouelian *et al.*, 2015; Huang *et al.*, 2018; Smith *et al.*, 2020).

Approaches used include assembly from histological sections (e.g., Hofstadler-Deiques *et al.*, 2005; Oisi *et al.*, 2015), CT scanning (e.g., Tse *et al.*, 2015; Krings *et al.*, 2017; Tesařová *et al.*, 2019; Zheng *et al.*, 2020; Kaczmarek *et al.*, 2020), or hypothetical and schematic models (e.g., Lee *et al.*, 2010; Manuel *et al.*, 2014; Menapace *et al.*, 2020). Cartilage is not always well represented by x-rays even when using contrast stains such as iodine or phosphotungstic acid (e.g., Metscher, 2009; Gignac *et al.*, 2015; Jones *et al.*, 2019), but achieving greater differentiation of cartilage is possible (Krings, *et al.*, 2017a; Zheng *et al.*, 2020; Gabner *et al.*, 2020). For some subjects, magnetic resonance imaging may be appropriate (Tse *et al.*, 2015; Dutel *et al.*, 2019).

Once the shape of the model is finalised, it is subdivided into very many simply shaped discrete elements (e.g., hexahedra, tetrahedra) that mathematically approximate the deformation of the geometry under loading (Fagan, 1996; Dar, 2002; Richmond *et al.*, 2005; Rayfield, 2007). If the number of elements with respect to the dimension of the structure of interest (mesh density) is insufficient, the analysis will incorrectly predict the deformation of the model and fail to resolve strain “hotspots” (Bright & Rayfield, 2011a).

### Material properties

Before performing the analysis, the material properties of the model must be specified, in particular Young's modulus (E) (resistance to deformation, commonly referred to as stiffness), and the degree of compression or expansion of the material in the direction perpendicular to loading, Poisson's ratio ( $\nu$ ). Ideally, the values used should correspond as closely as possible to material properties of the anatomical component being modelled. However, the range of material properties used may be limited by the software used and computer processing capacity.

Bones and teeth are often given uniform material properties comprising a Young's modulus value between 8,000 MPa (Zhang *et al.*, 2001; Tse *et al.*, 2015) and 17,000 MPa (Kupczik *et al.*, 2007; Gröning *et al.*, 2011; Curtis *et al.*, 2013). Material properties of bone within the same skull can show significant variation (e.g., Cuff *et al.*, 2015), and variable bone properties can be included within finite element models (e.g., McHenry *et al.*, 2007; Davis *et al.*, 2011; Chamoli & Wroe, 2011). However, the degree of variation within bone is drastically different from that between bone and cartilage. Therefore, representing cartilage and the cranial sutures which hold the bones together may be more important than representing the variation within bones. Sutures, if included in a model, are typically given a value of 20 MPa and



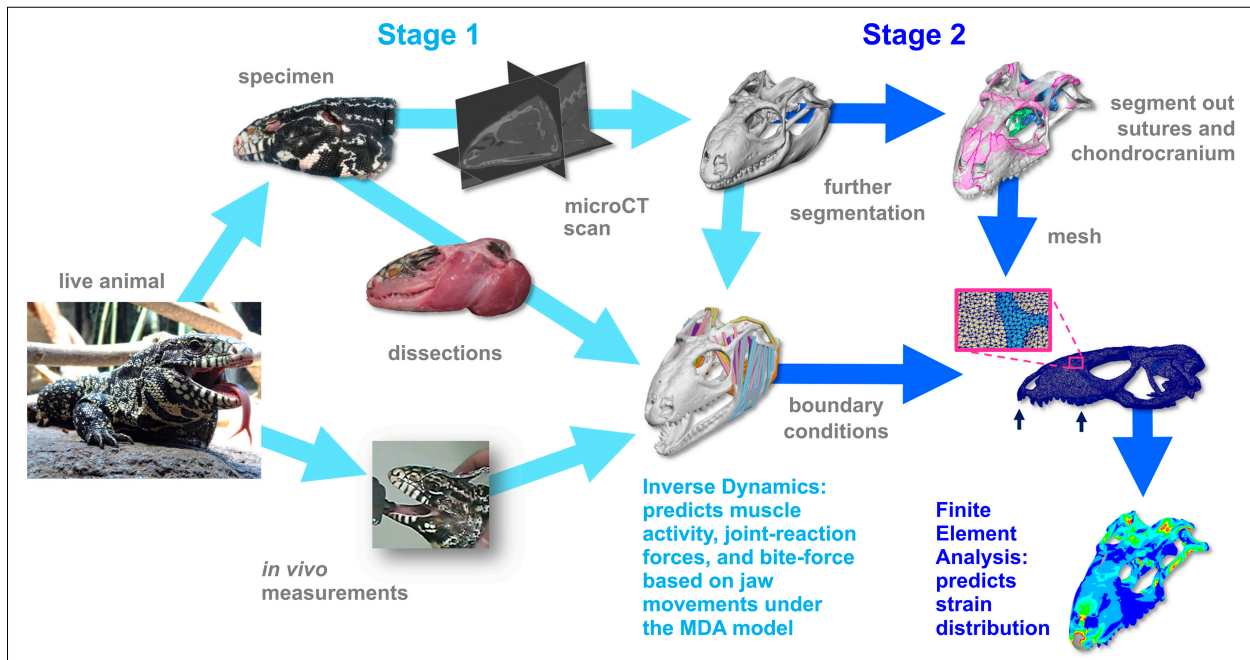


**Fig. 3.** A protocol for *in silico* biomechanical analysis of the skull of the lizard *Salvator merianae* (GRÖNING *et al.*, 2013; JONES *et al.*, 2017). Stage 1 involves multibody dynamics analysis (MDA) to establish likely loading (boundary) conditions whereas stage 2 involves a finite element analysis (FEA) to predict strain distribution. Image attributions: live animal, Bjørn Christian Tørrissen via Wikimedia Commons (CC BY-SA 3.0); *in vivo* measurements, Anthony Herrel; other images, the authors.

due to size constraints may be slightly enlarged relative to actual size (KUPCZIK *et al.*, 2007; JONES *et al.*, 2017). Cartilage, when included in models, has been given different values that are generally related to the species and anatomical region being analysed (WROE *et al.*, 2008; LEE *et al.*, 2010; LEARY *et al.*, 2015; JONES *et al.*, 2017).

Like bones, cartilage models tend to be given uniform material properties (e.g., LEE *et al.*, 2010; LEARY *et al.*, 2015; JONES *et al.*, 2017) but multiple values have been used to represent regional variation (WROE *et al.*, 2008). Models of nasal cartilage have been given low stiffness values, e.g., 0.8 MPa (LEARY *et al.*, 2015). However, the values used have generally been greater than those typically measured from fresh tissues (e.g., GRIFFIN *et al.*, 2016a). To accommodate uncertainty, a range of values can be used in different analyses to bracket the likely true value (DAR, 2002; JONES *et al.*, 2017). Nevertheless, when using a model with a single homogenous material property, alterations to the specified material property may make little difference to strain distribution, only magnitude (JONES *et al.*, 2017). The cartilage may also be given the same values as bone to provide a control or baseline comparison (WROE *et al.*, 2008; JONES *et al.*, 2017). For chondrichthyan tessellate cartilage a range of material property values has been used (WROE *et al.*, 2008: 10 to 7047 MPa).

Analysing how the cartilage components of biomechanical models behave under high strain is challenging because of the non-linear stress-strain-time relationships in cartilage (COHEN *et al.*, 1998; MENAPACE *et al.*, 2020; CUTCLIFFE & DEFRATE, 2020). Repetitive loading, such as in chewing, may also result in an evolution of proper-

ties during the process; something used by some material testing scientists as ‘preconditioning’ as it results in more uniform and repeatable measurements. It is possible to model and analyse this viscoelastic behaviour but it adds further complexity to the model and may be computationally intensive (COHEN *et al.*, 1998; HU *et al.*, 2003; TSE *et al.*, 2015; HUANG *et al.*, 2018).

### Loading and boundary conditions

The loading and constraints used in the model must be appropriate for the question being investigated (ROSS, 2005; RAYFIELD, 2007; PORRO *et al.*, 2013; MARCÉ-NOGUÉ *et al.*, 2015). To examine how different shaped nasal cartilages respond to nose tip depression the loading can be very simple (LEE *et al.*, 2010; LEARY *et al.*, 2015): anteroposterior deformation. However, to analyse the role of the chondrocranium in the context of the entire skull the loading is necessarily much more complex. One approach is to estimate the loading from the muscles and bite reaction forces using a detailed representation of the muscles and multibody dynamics analysis (CURTIS *et al.*, 2010; GRÖNING *et al.*, 2013). This method ensures that the muscle loading and bite reaction forces are in equilibrium, reducing the need for the (incorrect) application of a rigid constraint at a connection point between the skull and neck (MOAZEN *et al.*, 2008).

### Validation

To understand the usefulness or limitations of a biomechanical model it is necessary to compare model output

**Table 1.** Example material properties recorded for various samples of cartilage. Note that the lower values reported in JIN & LEWIS (2004) represent the initial response.

Material	Taxon	Genus	species	Sample	Young Modulus (E) MPa	Poisson Ratio (ν)	Reference
Cartilage	Human	<i>Homo</i>	<i>sapiens</i>	Nasal cartilage (medial)	0,44	na	Richmon et al. 2006
Cartilage	Cow	<i>Bos</i>	<i>taurus</i>	Articular cartilage (patella)	0,45	0,46	Jin and Lewis 2004
Cartilage	Rabbit – 6 – 9 months	<i>Oryctolagus</i>	<i>cuniculus</i>	Articular cartilage (tibia, lateral)	0,53	na	Hoch et al 1983
Cartilage	Human	<i>Homo</i>	<i>sapiens</i>	Nasal cartilage (rostrocaudal)	0,66	na	Richmon et al. 2006
Cartilage	Rabbit – 19 months	<i>Oryctolagus</i>	<i>cuniculus</i>	Articular cartilage (tibia, lateral)	0,66	na	Hoch et al 1983
Cartilage	Human	<i>Homo</i>	<i>sapiens</i>	Nasal cartilage (dorsoventral)	0,71	na	Richmon et al. 2006
Cartilage	Rabbit – 6 – 9 months	<i>Oryctolagus</i>	<i>cuniculus</i>	Articular cartilage (tibia, medial)	0,76	na	Hoch et al 1983
Cartilage	Rabbit – 19 months	<i>Oryctolagus</i>	<i>cuniculus</i>	Articular cartilage (tibia, medial)	0,81	na	Hoch et al 1983
Cartilage	Human	<i>Homo</i>	<i>sapiens</i>	Nasal cartilage	0,98	na	Griffin et al 2016a
Cartilage	Human	<i>Homo</i>	<i>sapiens</i>	Auricular cartilage (helix)	1,41	na	Griffin et al 2016b
Cartilage	Human	<i>Homo</i>	<i>sapiens</i>	Auricular cartilage (tragus)	1,67	na	Griffin et al 2016b
Cartilage	Human	<i>Homo</i>	<i>sapiens</i>	Auricular cartilage (antihelix)	1,71	na	Griffin et al 2016b
Cartilage	Human	<i>Homo</i>	<i>sapiens</i>	Auricular cartilage (anti-tragus)	1,79	na	Griffin et al 2016b
Cartilage	Cow	<i>Bos</i>	<i>taurus</i>	Articular cartilage (patella)	1,79	0,53	Jin and Lewis 2004
Cartilage	Cow	<i>Bos</i>	<i>taurus</i>	Nasal cartilage	2,03	0,24	Columbo et al. 2013
Cartilage	Human	<i>Homo</i>	<i>sapiens</i>	Alar cartilage	2,06	na	Griffin et al 2016a
Cartilage	Human	<i>Homo</i>	<i>sapiens</i>	Auricular cartilage (concha)	2,08	na	Griffin et al 2016b
Cartilage	Human	<i>Homo</i>	<i>sapiens</i>	Alar cartilage	2,12	na	Griffin et al 2016a
Cartilage	Human	<i>Homo</i>	<i>sapiens</i>	Septal cartilage	2,50	na	Griffin et al 2016a
Cartilage	Human	<i>Homo</i>	<i>sapiens</i>	Septal cartilage	2,74	na	Griffin et al 2016a
Cartilage	Human	<i>Homo</i>	<i>sapiens</i>	Auricular cartilage (tragus)	2,80	na	Zahert et al. 2000
Cartilage	Human	<i>Homo</i>	<i>sapiens</i>	Auricular cartilage (concha)	3,40	na	Zahert et al. 2000
Cartilage	Human	<i>Homo</i>	<i>sapiens</i>	Septal cartilage	3,47	na	Griffin et al 2016a
Cartilage	Cow	<i>Bos</i>	<i>taurus</i>	Articular cartilage (femur)	5,00	na	Peters et al 2017
Mineralised cartilage	Human	<i>Homo</i>	<i>sapiens</i>	Articular cartilage (femur)	19,00	na	Ferguson et al. 2003
Mineralised cartilage	Gulper shark	<i>Centrophorus</i>	<i>granulosus</i>	Vertebral cartilage	20,00	na	Porter et al. 2006
Mineralised cartilage	Torpedo ray	<i>Tetronarce</i>	<i>californica</i>	Vertebral cartilage	25,50	na	Porter et al. 2006
Mineralised cartilage	Short finned mako	<i>Isurus</i>	<i>oxyrinchus</i>	Vertebral cartilage	329,40	na	Porter et al. 2006
Mineralised cartilage	Sandbar shark	<i>Carcharhinus</i>	<i>plumbeus</i>	Vertebral cartilage	396,90	na	Porter et al. 2006
Mineralised cartilage	Gulper shark	<i>Centrophorus</i>	<i>granulosus</i>	Vertebral cartilage	425,80	na	Porter et al. 2006
Mineralised cartilage	Smooth hammerhead	<i>Sphyma</i>	<i>zygaena</i>	Vertebral cartilage	523,40	na	Porter et al. 2006
Mineralised cartilage	Silky shark	<i>Carcharhinus</i>	<i>falciformis</i>	Vertebral cartilage	563,90	na	Porter et al. 2006

to other sources of data. For computer-generated biomechanical skull models, “validation” can be obtained by comparisons to *in vivo* bite force performance (Fig. 3, GRÖNING *et al.*, 2013; SELLERS *et al.*, 2017), *in vivo* muscle activity (CURTIS *et al.*, 2010), or *in vivo* and *ex vivo* strain (REMLER, 1998; CARTER & WONG, 2003; BRIGHT & RAYFIELD, 2011b; BRIGHT & GRÖNING, 2011; GRÖNING *et al.*, 2012; PORRO *et al.*, 2013, 2014; CUFF *et al.*, 2015). These validation approaches are easier for some species than they are for others. Bite force performance can be estimated by encouraging test subjects to bite on custom bite force transducers (e.g., DESSEM & DRUZINSKY, 1992; PAPHANGKORAKIT & OSBORN, 1998; HERREL *et al.*, 1999; ANDERSON *et al.*, 2008; LAPPIN & JONES, 2014; VAN VUUREN *et al.*, 2020). This approach has been used successfully for a range of taxa, notably crocodylians, lizards, bats, and rodents but also sharks (DESSEM & DRUZINSKY, 1992; HERREL *et al.*, 1999; HUBER *et al.*, 2005; BECERRA *et al.*, 2011; ERICKSON *et al.*, 2012; LAPPIN & JONES, 2014; LAPPIN *et al.*, 2017; JONES *et al.*, 2020). Muscle activity can be measured using electromyography (LOEB *et al.*, 1986; DESSEM & DRUZINSKY, 1992) although the relationships between EMG measurements and actual force remain problematic to determine with certainty. Surface strain can be measured using strain gauges (BUCKLAND-WRIGHT, 1978; ROSS & HYLANDER, 1996; THOMASON, *et al.*, 2001; ROSS & METZGER, 2004; BRIGHT & RAYFIELD, 2011b; CUFF *et al.*, 2015) or electronic speckle pattern interferometry (BRIGHT & GRÖNING, 2011; GRÖNING *et al.*, 2012). Internal strain can be measured using loading within a CT scanner (EVANS *et al.*, 2012).

Due to the possibility of intraspecific variation, comparisons should ideally be specimen-specific (GRÖNING *et al.*, 2013). Also, as cautioned by LAPPIN & JONES (2014), “if model predictions do not match *in vivo* data there are three possibilities *prima facie*: the model is in error, the *in vivo* data are in error, or both are in error.” It should not be assumed that estimates of strain or bite force performance collected *in vivo* are 100% correct. Even when biomechanical models and empirical data do correspond, it can be due to chance alone (NIKLAS, 1992; ALEXANDER, 2003). Hence, multiple parallel comparisons and sensitivity analyses are desirable.

### Example Finite Element Analyses of chondrocrania

To date, only a handful of studies have used computer modelling to examine the biomechanics of chondrocranial structures. Most of these have focused on the nasal cartilage in humans (e.g., LEE *et al.*, 2010; MANUEL *et al.*, 2014; SHAMOUELIAN *et al.*, 2015; TSE *et al.*, 2015; LEARY *et al.*, 2015; HUANG *et al.*, 2018), but there has also been one focused on a tegu lizard (JONES *et al.*, 2017) and another study of possible relevance on the great white shark (WROE *et al.*, 2008).

Analyses of humans have identified where strains might concentrate in nasal cartilages of particular shapes when the nose is depressed (e.g., LEE *et al.*, 2010; MA-

NUEL *et al.*, 2014; LEARY *et al.*, 2015). They have also helped identify the relationship between loading and deformations associated with cleft lip (HUANG *et al.*, 2018). Models investigating hypothetical traumatic anterior impacts suggest that, at least in humans, the nasal cartilage can absorb significant amounts of impact energy that might otherwise damage the brain (e.g., LEE *et al.*, 2010; TSE *et al.*, 2015). To date, most studies have modelled the nasal cartilage as linear elastic (e.g., MANUEL *et al.*, 2014; LEARY *et al.*, 2015; TSE *et al.*, 2015; MENAPACE *et al.*, 2020) but future work is likely to pursue more accurate representation (MENAPACE *et al.*, 2020).

In the adult black and white tegu lizard, *Salvator merianae*, the chondrocranium was found to have little impact on the strain generated from anterior or posterior biting regardless of material properties used (JONES *et al.*, 2017). When the chondrocranium was modelled as bone (17,000 MPa), strains were lower in some regions of the cranium but only slightly (JONES *et al.*, 2017). Within the chondrocranium itself, strains were twice as large during anterior biting compared to posterior biting (JONES *et al.*, 2017). Moreover, for both anterior and posterior biting, the greatest strains were located anteriorly rather than posteriorly, and these were tensile rather than compressive (JONES *et al.*, 2017). These results do not suggest that the chondrocranium provides a vertical support structure in lizards (MOSS *et al.*, 1968; STENSTRÖM & THILANDER, 1970; KEMBLE, 1973). Perhaps this result is not surprising given the maturity of the animal used in the analysis and the huge difference in the material properties of bone and cartilage. It remains possible that the chondrocranium has a greater role in juvenile or paedomorphic lizards. Moreover, the chondrocranium is also still likely important for supporting the eye and associated muscles (PEARSON, 1921).

A biomechanical analysis of biting in the great white shark, *Carcharodon carcharias*, did not measure strain in the chondrocranium but it did examine stress and strain in the tessellated cartilage jaws (WROE *et al.*, 2008). Analyses found that despite being less stiff than a model given the material properties of bone, the jaws could still apply significant bite forces, as previous bite force estimates from other sharks might suggest (HUBER *et al.*, 2005). These results provide further evidence that cartilage can represent a support material when adequately mineralised.

## Discussion

The chondrocranium is highly variable among vertebrates and this variation may reflect its function and biomechanical role. To date, its biomechanical role remains poorly known in most taxa. The extreme replacement of the chondrocranium with bone in amniotes is associated with greater rigidity of the skull and any flexion restricted to a small number of specific zones (DE BEER, 1930; KAUCKA & ADAMEYKO, 2019). Cartilage is less stiff than

bone and may, therefore, seem less suitable for use in levers, applying bite force, or resisting feeding loads. Amniotes, which generally employ powered bites, may have sophisticated oral food processing (REILLY *et al.*, 2001; ROSS *et al.*, 2009; JONES *et al.*, 2012), and often retain only a small fraction of the chondrocranium as cartilage. Nevertheless, the jaw muscles of hagfish (which lack bone) are estimated to generate similar forces to those of gnathostomes (CLARK & SUMMERS, 2007) and tadpoles can pursue carnivorous and even macrophagous diets with minimal mineralisation and replacement by bone (e.g., CANDIOTI, 2007; HAAS *et al.*, 2014; KLINGER-STROBEL *et al.*, 2020). With their mineralised cartilage, chondrichthyan fish can attain large body sizes and employ great bite forces (HUBER *et al.*, 2005; WROE *et al.*, 2008). Moreover, complex oral food processing is not restricted to amniotes (e.g., HEISS *et al.*, 2019).

In mammals the location of the chondrocranium along the long axis of the snout and the results of its experimental removal in the young have led to suggestions that it might provide a vertical strut that serves to resist compressive loading (MOSS *et al.*, 1968; STENSTRÖM & THILANDER, 1970; KEMBLE, 1973). Alternatively, measurements of *in vivo* strain and comparisons of material properties in pigs raised the possibility that the chondrocranium is involved in dampening strain within the snout (AL DAYEH *et al.*, 2009; AL DAYEH & HERRING, 2014; LEE *et al.*, 2010). In humans the nasal cartilage clearly provides some support to the nose, and its capacity to deform may be useful for accommodating some forms of trauma (LEE *et al.*, 2010; TSE *et al.*, 2015). The general relationships between nose shape, regional climate, and sexual attraction and communication in humans remain unclear and controversial (CALDER & YOUNG, 2005; MIKALSEN *et al.*, 2014; ZAIDI *et al.*, 2018), but disruption to the nasal cartilage can impact individual life quality (GRIFFIN *et al.*, 2016a; LAVERNIA *et al.*, 2019). Therefore, understanding the biomechanical properties of this part of the chondrocranium may improve the potential of aesthetic, corrective, and reconstructive surgery (GRIFFIN *et al.*, 2016a; LAVERNIA *et al.*, 2019). Biomechanical modelling of the chondrocranium in lizards did not support the hypothesis that it represents a load bearing vertical strut (JONES *et al.*, 2017). However, the lizard modelled, the South American tegu, *Salvator merianae*, was a very heavily built adult. It is possible that the chondrocranium is more important in small or juvenile lizards (HALLERMANN, 1992).

Computer-based analyses provide the potential for parallel analyses of different taxa, different life stages, and hypothetical models that could establish the relationship between observed morphological variation and biomechanical performance. The material properties of cartilage are challenging to model but the potential to gather empirical data is increasing (LAKIN *et al.*, 2017). When modelling parts of the chondrocranium with the skull, one issue that requires attention is how to model the connection between the bone and cartilage. The nature of the interface between the skull and nasal cartilage appears relatively poorly known (HAFKAMP *et al.* 1999).

In pigs it was found to differ between regions (AL DAYEH & HERRING, 2009): the connection between the nasal cartilage and premaxilla, nasal, and frontal bones was fibrous, but a pad of loose connective tissue connected the same cartilage to the vomer. How the interface between the two materials is modelled will affect how strains are transferred between them and in turn the overall strain distributions. Connections between different parts of the nasal cartilage may also be important (SHAMOUELIAN *et al.*, 2015).

Understanding the sources of biological variation is a core goal of the biological sciences. Therefore, as well as improvement to model detail and validation, a wider range of vertebrate subjects should be examined, in particular larvae, juveniles, and very small adult animals.

## Acknowledgements

We thank Ingmar Werneburg for organising the symposium, Casey Holliday, Matt Friedman, Alice Clement, and Kyle Armstrong for discussion, Ruben Guzman-Gutierrez and Ralf Britz for help accessing literature, and Hendrik Müller and Juan Daza for constructive comments during peer review. We thank the Biotechnology and Biological Sciences Research Council (BBSRC) who provided funding for this research (BB/H011854/1; BB/H011668/1; BB/H011390/1; BB/M010287/1; BB/M008525/1; BB/M008061/1) and a Discovery Early Career Researcher Award DE130101567 (Australian Research Council) which supported MEHJ.

## References

- ABITUA, P. B., WAGNER, E., NAVARRETE, I. A. & LEVINE, M. (2012). Identification of a rudimentary neural crest in a non-vertebrate chordate. *Nature*, **492**, 104–107.
- AHLBERG, P. E., CLACK, J. A. & LUKŠEVIČS, E. (1996). Rapid braincase evolution between *Panderichthys* and the earliest tetrapods. *Nature*, **381**, 61–64.
- AL DAYEH, A. A. & HERRING, S. W. (2014). Compressive and tensile mechanical properties of the porcine nasal septum. *Journal of Biomechanics*, **40**, 154–161.
- AL DAYEH, A. A., RAFFERY, K. L., EGBERT, M. & HERRING, S. W. (2009). Deformation of nasal septal cartilage during mastication. *Journal of Morphology*, **270**, 1209–1218.
- ALEXANDER, R. M. (2003). Modelling approaches in biomechanics. *Philosophical Transactions of the Royal Society of London B*, **358**, 1429–1435.
- ALLIS JR, E. P. (1897). The morphology of the petrosal bone and of the sphenoidal region of the skull of *Amia calva*. *Zoological Bulletin*, **1**, 1–26.
- ALLIS JR, E. P. (1922). The cranial anatomy of *Polypterus*, with special reference to *Polypterus bichir*. *Journal of Anatomy*, **56** (3–4), 1–189.
- ANDERSON, R. A., MCBRAYER, L. D. & HERREL, A. (2008). Bite force in vertebrates: opportunities and caveats for use of a nonpareil whole-animal performance measure. *Biological Journal of the Linnean Society*, **93**, 709–720.
- ASPDEN, R. M. (1990). Constraining the lateral dimensions of uniaxially loaded materials increases the calculated strength and stiffness: application to muscle and bone. *Journal of Material Science: Materials in Medicine*, **1**, 100–104.

- ASPDEN, R. M. (1994). Fibre reinforcing by collagen in cartilage and soft connective tissues. *Proceedings of the Royal Society of London B*, **258**, 195–200.
- ATKINS, J. B., REISZ, R. R. & MADDIN, H. C. (2019). Braincase simplification and the origin of lissamphibians. *PLoS ONE*, **14**, e0213694.
- BASDEN, A. M., YOUNG, G. C., COATES & M. I. & RITCHIE, A. (2000). The most primitive osteichthyan braincase? *Nature*, **403**, 185–188.
- BECERRA, F., ECHEVERRÍA, A., VASSALLO, A. I. & CASINOS, A. (2011). Bite force and jaw biomechanics in the subterranean rodent *Talpa talpa* (Ctenomyidae: Octodontidae). *Canadian Journal of Zoology*, **89**, 334–342.
- BERGLAND, O. & BORCHGREVINK, H. (1974). The role of the nasal septum in midfacial growth in man elucidated by the maxillary development in certain types of facial clefts: a preliminary report. *Scandinavian Journal of Plastic and Reconstructive Surgery*, **8**, 42–48.
- BELLAIRS, A. D'A. & KAMAL, A. M. (1981). The chondrocranium and the development of the skull in recent reptiles, pp. 1–283 in: GANS, C. & PARSONS, T. S. (eds) *Biology of the Reptilia, Volume 11, Morphology F*. New York, Academic Press.
- BENJAMIN, M. (1990). The cranial cartilages of teleosts and their classification. *Journal of Anatomy*, **169**, 153–172.
- BOURKE, J. M. & WITMER, L. M. (2016). Nasal conchae function as aerodynamic baffles: experimental computational fluid dynamic analysis in a turkey nose (Aves: Galliformes). *Respiratory Physiology & Neurobiology*, **234**, 32–46.
- BOYD, R. B. (1975). A gross and microscopic study of the respiratory anatomy of the Antarctic Weddell seal, *Leptonychotes weddellii*. *Journal of Morphology*, **147**, 309–335.
- BRAZEAU, M., GILES, S., DEARDEN, R., JERVE, A., ARIUNCHIMEG, Y., ZORIG, E., GUILLERME, T. & CASTIELLO, M. (2020). Endochondral bone in an Early Devonian 'placoderm' from Mongolia. *bioRxiv*, <https://doi.org/10.1101/2020.06.09.132027>.
- BRIGHT, J. A. & RAYFIELD, E. J. (2011a). The response of cranial biomechanical finite element models to variations in mesh density. *Anatomical Record*, **294**, 610–620.
- BRIGHT, J. A. & RAYFIELD, E. J. (2011b). Sensitivity and *ex vivo* validation of finite element models of the domestic pig cranium. *Journal of Anatomy*, **219**, 456–471.
- BRIGHT, J. A. & GRÖNING, F. (2011). Strain accommodation in the zygomatic arch of the pig: A validation study using digital speckle pattern interferometry and finite element analysis. *Journal of Morphology*, **272**, 1388–1398.
- BRUINJES, T. D., VAN OLPHEN, A. F., HILLEN, B. & HUIZING, E. H. (1998). A functional anatomic study of the relationship of the nasal cartilages and muscles to the nasal valve area. *Laryngoscope*, **108**, 1025–1032.
- BUCKLAND-WRIGHT, J. C. (1978). Bone structure and the patterns of force transmission in the cat skull (*Felis catus*). *Journal of Morphology*, **155**, 35–61.
- BURGIN, L. V. (2003). *Impact Loading of Articular Cartilage*. PhD Thesis, Aberdeen, University of Aberdeen.
- BURGIN, L. V., EDELSTEN, L. & ASPDEN, R. M. (2014). The mechanical and material properties of elderly human articular cartilage subject to impact and slow loading. *Medical Engineering and Physics*, **36**, 226–232.
- CALDER, A. J. & YOUNG, A. W. (2005). Understanding the recognition of facial identity and facial expression. *Nature Reviews Neuroscience*, **6**, 641–651.
- CANDIOTI, M. F. V. (2007). Anatomy of anuran tadpoles from lentic water bodies: systematic relevance and correlation with feeding habits. *Zootaxa*, **1600**, 1–175.
- CARTER, D. R. & WONG, M. (2003). Modelling cartilage mechanobiology. *Philosophical Transactions of the Royal Society of London B*, **358**, 1461–1471.
- CHAMOLI, U. & WROE, S. (2011). Allometry in the distribution of material properties and geometry of the felid skull: why larger species may need to change and how they may achieve it. *Journal of Theoretical Biology*, **283**, 217–226.
- CHANG, B., REIGHARD, C., FLANAGAN, C., HOLLISTER, S. & ZOPF, D. (2020). Evaluation of human nasal cartilage nonlinear and rate dependent mechanical properties. *Journal of Biomechanics*, **100**, 109549.
- CLACK, J. A. (1998). The neurocranium of *Acanthostega gunnari* Jarvik and the evolution of the otic region in tetrapods. *Zoological Journal of the Linnean Society*, **122**, 61–97.
- CLARK, A. J. & SUMMERS, A. P. (2007). Morphology and kinematics of feeding in hagfish: possible functional advantages of jaws. *Journal of Experimental Biology*, **210**, 3897–3909.
- CLEMENT, A. M. & AHLBERG, P. E. (2014). The first virtual cranial endocast of a lungfish (Sarcopterygii: Dipnoi). *PLoS ONE*, **9**, e113898.
- COATES, M. I., GESS, R. W., FINARELLI, J. A., CRISWELL, K. E. & TIETJEN, K. (2017). A symmoriiform chondrichthyan braincase and the origin of chimaeroid fishes. *Nature*, **541**, 208–211.
- COHEN, B., LAI, W. M. & MOW, V. C. (1998). A transversely isotropic biphasic model for unconfined compression of growth plate and chondroepiphysis. *Journal of Biomechanical Engineering*, **120**, 491–496.
- COLE, A. G. (2011). A review of diversity in the evolution and development of cartilage: the search for the origin of the chondrocyte. *European Cells and Materials*, **21**, 122–129.
- COLE, A. G. & HALL, B. K. (2004a). Cartilage is a metazoan tissue; integrating data from nonvertebrate sources. *Acta Zoologica*, **85**, 69–80.
- COLE, A. G. & HALL, B. K. (2004b). The nature and significance of invertebrate cartilages revisited: distribution and histology of cartilage and cartilage-like tissues within the Metazoa. *Zoology*, **107**, 261–273.
- COLUMBO, V., ČADOVÁ, M. & GALLO, L. M. (2013). Mechanical behaviour of bovine nasal cartilage under static and dynamic loading. *Journal of Biomechanics*, **46**, 2137–2144.
- COPRAY, J. C. (1986). Growth of the nasal septal cartilage of the rat *in vitro*. *Journal of Anatomy*, **144**, 99–111.
- COULY, G. F., COLTEY, P. M. & LE DOUARIN, N. M. (1993). The triple origin of skull in higher vertebrates: a study in quail-chick chimeras. *Development*, **117**, 409–429.
- COURTLAND, H. W., WRIGHT, G. M., ROOT, R. G. & DEMONT, M. E. (2003). Comparative equilibrium mechanical properties of bovine and lamprey cartilaginous tissues. *Journal of Experimental Biology*, **206**, 1397–1408.
- CUFF, A. R., BRIGHT, J. A. & RAYFIELD, E. J. (2015). Validation experiments on finite element models of an ostrich (*Struthio camelus*) cranium. *PeerJ*, **3**, e1294.
- CUNDALL, D. & SHARDO, J. (1995). Rhinokinetic snout of thamnophiine snakes. *Journal of Morphology*, **225**, 31–50.
- CURTIS, A. A. & SIMMONS, N. B. (2018). Prevalence of mineralized elements in the rostra of bats (Mammalia: Chiroptera). *Journal of Mammalogy*, **99**, 1387–1397.
- CURTIS, N. (2011). Craniofacial biomechanics: an overview of recent multibody modelling studies. *Journal of Anatomy*, **218**, 16–25.
- CURTIS, N., JONES, M. E. H., EVANS, S. E., O'HIGGINS, P. & FAGAN, M. J. (2013). Cranial sutures work collectively to distribute strain throughout the reptile skull. *Journal of the Royal Society Interface*, **10**, 20130442.
- CURTIS, N., JONES, M. E. H., EVANS, S. E., SHI, J., O'HIGGINS, P. & FAGAN, M. J. (2010). Predicting muscle activation patterns from motion and anatomy: modelling the skull of *Sphenodon* (Diapsida: Rhynchocephalia). *Journal of the Royal Society Interface*, **7**, 153–160.
- CURTIS, N., JONES, M. E. H., SHI, J., O'HIGGINS, P., EVANS, S. E. & FAGAN, M. J. (2011a). Functional relationship between skull form and feeding mechanics in *Sphenodon*, and implications for diapsid skull development. *PLoS ONE*, **6**, e29804.
- CURTIS, N., WITZEL, U., FITTON, L., O'HIGGINS, P. & FAGAN, M. (2011b). The mechanical significance of the temporal fasciae in *Macaca fascicularis*: an investigation using Finite Element Analysis. *Anatomical Record*, **294**, 1178–1190.

- CUTCLIFFE, H. C. & DEFRADE, L. E. (2020). Comparison of cartilage mechanical properties measured during creep and recovery. *Scientific Reports*, **10**, 1–8.
- DAR, F. H., MEAKIN J. R., ASPDEN R. M. (2002). Statistical methods in finite element analysis. *Journal of Biomechanics*, **35**, 1155–1161.
- DAVIS, J. L., DUMONT, E. R., STRAIT, D. S. & GROSSE, I. R. (2011). An efficient method of modeling material properties using a thermal diffusion analogy: an example based on craniofacial bone. *PLoS ONE*, **6**, e17004.
- DE BEER, G. R. (1930). The early development of the chondrocranium of the lizard. *Quarterly Journal of Microscopical Science*, **73**, 606–739.
- DE BEER, G. R. (1937). *The Development of the Vertebrate Skull*. Oxford, Oxford University Press.
- DEAN, M. N. & SUMMERS, A. P. (2006). Mineralized cartilage in the skeleton of chondrichthyan fishes. *Zoology*, **109**, 164–168.
- DESSEM, D. & DRUZINSKY, R. E. (1992). Jaw-muscle activity in ferrets, *Mustela putorius furo*. *Journal of Morphology*, **213**, 275–286.
- DONOGHUE, P. C. J., SANSOM, I. J. & DOWNS, J. P. (2006). Early evolution of vertebrate skeletal tissues and cellular interactions, and the canalization of skeletal development. *Journal of Experimental Zoology*, **306**, 278–294.
- DONOGHUE, P. C. J., GRAHAM, A. & KELSH, R. N. (2008). The origin and evolution of the neural crest. *BioEssays*, **30**, 530–541.
- DOWNS, J. P., DAESCHLER, E. B., JENKINS, F. A. & SHUBIN, N. H. (2008). The cranial endoskeleton of *Tiktaalik roseae*. *Nature*, **455**, 925–929.
- DUTEL, H., GALLAND, M., TAFFOREAU, P., LONG, J. A., FAGAN, M. J., JANVIER, P., HERREL, A., SANTIN, M. D., CLÉMENT, G. & HERBIN, M. (2019). Neurocranial development of the coelacanth and the evolution of the sarcopterygian head. *Nature*, **569**, 556–559.
- EBENSTEIN, D. M. & PRUITT, L. A. (2006). Nanoindentation of biological materials. *Nano Today*, **1**, 26–33.
- EDELSTEN, L., JEFFREY, J. E., BURGIN, L. V. & ASPDEN, R. M. (2010). Viscoelastic deformation of articular cartilage during impact loading. *Soft Matter*, **6**, 5206–5212.
- ERICKSON, G. M., GIGNAC, P. M., STEPPAN, S. J., LAPPIN, A. K., VLIET, K. A., BRUEGGEN, J. D., INOUE, B. D., KLEDZIK, D. & WEBB, G. J. (2012). Insights into the ecology and evolutionary success of crocodylians revealed through bite-force and tooth-pressure experimentation. *PLoS ONE*, **7**, e31781.
- EVANS, S. E. (2008). The skull of lizards and tuatara, pp. 1–344 In: GANS, C., GAUNT, A. S. & ADLER K. (eds) *Biology of the Reptilia, Vol. 20, Morphology H*. Ithaca, New York, Society for the Study of Amphibians and Reptiles.
- EVANS, S. P., PARR, W. C. H., CLAUSEN, P. D., JONES, A. & WROE, S. (2012). Finite element analysis of a micromechanical model of bone and a new 3D approach to validation. *Journal of Biomechanics*, **45**, 2702–2705.
- FAGAN, M. J. (1996). *Finite Element Analysis*. Upper Saddle River, NJ, Prentice Hall.
- FERGUSON, V. L., BUSHBY, A. J. & BOYDE, A. (2003). Nanomechanical properties and mineral concentration in articular calcified cartilage and subchondral bone. *Journal of Anatomy*, **203**, 191–202.
- FERNANDEZ BLANCO, M. V. (2019). Development of the chondrocranium of two caiman species, *Caiman latirostris* and *Caiman yacare*. *Journal of Anatomy*, **234**, 899–916.
- FISH, J. L. (2019). Evolvability of the vertebrate craniofacial skeleton. *Seminars in Cell & Developmental Biology*, **91**, 13–22.
- FLAM, E. (1974). The tensile and flexural properties of bovine nasal cartilage. *Journal of Biomedical Materials Research*, **8**, 277–282.
- FOREY, P. (1998). *History of Coelacanth Fishes*. London, Chapman & Hall.
- GABNER, S., BÖCK, P., FINK, D., GLÖSMANN, M. & HANDSCHUH, S. (2020). The visible skeleton 2.0: phenotyping of cartilage and bone in fixed vertebrate embryos and fetuses based on x-ray microCT. *Development*, **147**, 11.
- GANGE, R. J. & JOHNSTON, L. E. (1974). The septopremaxillary attachment and midfacial growth: an experimental study on the albino rat. *American Journal of Orthodontics*, **66**, 71–81.
- GAUPP, E. (1900). Das Chondrocranium von *Lacerta agilis*. Ein Beitrag zum Verständnis des Amniotenschädels. *Anatomische Hefte. 1 Abteilung*, **14**, 434–594.
- GIGNAC, P. M., KLEY, N. J., CLARKE, J. A., COLBERT, M. W., MORHARDT, A. C., CERIO, D., COST, I. N., COX P. G., DAZA, J. D., EARLY, C. M., ECHOLS, M. S., HENKELMAN, R. M., HERDINA, A., N., HOLLIDAY, C., LI, Z., MAHLOW, K., MERCHANT, S., MÜLLER, J., ORSBON, C. P., PALUH, D. J., THIES, M. L., TSAI, H. P. & WITMER, L. M. (2016). Diffusible iodine-based contrast-enhanced computed tomography (diceCT): an emerging tool for rapid, high-resolution, 3-D imaging of metazoan soft tissues. *Journal of Anatomy*, **228**, 889–909.
- GILLIS, J. A. (2019). The development and evolution of cartilage, pp. 1–13 in: YELON, R. & MAYOR, R. (eds). *Elsevier Reference Module in Life Sciences: Developmental Biology*. Amsterdam, Elsevier.
- GÖBBEL, L. (2000). The external nasal cartilages in Chiroptera: significance for intraordinal relationships. *Journal of Mammalian Evolution*, **7**, 167–201.
- GRANDE, L. & BEMIS, W. E. (1998). A comprehensive phylogenetic study of amiid fishes (Amiidae) based on comparative skeletal anatomy. An empirical search for interconnected patterns of natural history. *Journal of Vertebrate Paleontology*, **18** (Supplement 1), 1–696.
- GRIFFIN, M. F., PREMAKUMAR, Y., SCIFALIAN, A. M., SZARKO, M. & BUTLER, P. E. M. (2016a). Biomechanical characterisation of the human nasal cartilages; implications for tissue engineering. *Journal of Materials Science: Materials in Medicine*, **27**, 1–6.
- GRIFFIN, M. F., PREMAKUMAR, Y., SEIFALIAN, A. M., SZARKO, M. & BUTLER, P. E. M. (2016b). Biomechanical characterisation of the human auricular cartilages; implications for tissue engineering. *Annals of Biomedical Engineering*, **44**, 3460–3467.
- GRÖNING, F., FAGAN, M. J. & O’HIGGINS, P. (2011). The effects of the periodontal ligament on mandibular stiffness: a study combining finite element analysis and geometric morphometrics. *Journal of Biomechanics*, **44**, 1304–1312.
- GRÖNING, F., BRIGHT, J. A., FAGAN, M. J. & O’HIGGINS, P. (2012). Improving the validation of finite element models with quantitative full-field strain comparisons. *Journal of Biomechanics*, **45**, 1498–1506.
- GRÖNING, F., JONES, M. E. H., CURTIS, N., HERREL, A., O’HIGGINS, P., EVANS, S. E. & FAGAN, M. J. (2013). The importance of accurate muscle modelling for biomechanical analyses: a case study with a lizard skull. *Journal of the Royal Society Interface*, **10**, 20130216.
- GUPTA, S., LIN, J., ASHBY, P. & PRUITT, L. (2009). A fiber reinforced poroelastic model of nanoindentation of porcine costal cartilage: a combined experimental and finite element approach. *Journal of the Mechanical Behavior of Biomedical Materials*, **2**, 326–338.
- HAAS, A., POHLMAYER, J., MCLEOD, D. S., KLEINTEICH, T., HERTWIG, S. T., DAS, I. & BUCHHOLZ, D. R. (2014). Extreme tadpoles II: the highly derived larval anatomy of *Occidozyga baluensis* (Boulenger, 1896), an obligate carnivorous tadpole. *Zoomorphology*, **133**, 321–342.
- HAFKAMP, H. C., BRUINTJES, T. D. & HUIZING, E. H. (1999). Functional anatomy of the premaxillary area. *Rhinology*, **37**, 21–24.
- HALLERMANN, J. (1992). Morphological significance of the orbito-temporal region in amphikinetid skulls of juvenile iguanians (Squamata). *Zoologische Jahrbücher, Abteilung für Anatomie und Ontogenie der Tiere*, **122**, 203–206.
- HEISS, E., SCHWARZ, D. & KONOW, N. (2019). Chewing or not? Intraoral food processing in a salamandrid newt. *Journal of Experimental Biology*, **222**, 1–12.
- HERNÁNDEZ-JAIMES, C., JEREZ, A. & RAMÍREZ-PINILLA, M. P. (2012). Embryonic development of the skull of the Andean lizard *Pty-*



- choglossus bicolor* (Squamata, Gymnophthalmidae). *Journal of Anatomy*, **221**, 285–302.
- HERREL, A., SPITHOVEN, L., VAN DAMME, R. & DE VREE, F. (1999). Sexual dimorphism of head size in *Gallotia galloti*: testing the niche divergence hypothesis by functional analyses. *Functional Ecology*, **13**, 289–297.
- HERRING, S. W. & TENG, S. (2000). Strain in the braincase and its sutures during function. *American Journal of Physical Anthropology*, **112**, 575–593.
- HILLENIUS, W. J. (1992). The evolution of nasal turbinates and mammalian endothermy. *Paleobiology*, **18**, 17–29.
- HILTON, E. J., GRANDE, L. & BEMIS, W. E. (2011). Skeletal anatomy of the shortnose sturgeon, *Acipenser brevirostrum* Lesueur, 1818, and the systematics of sturgeons (Acipenseriformes, Acipenseridae). *Fieldiana Life and Earth Sciences*, **2011**, 1–168.
- HILTON, W. A. (1950). Review of the chondrocranium of tailed amphibia. *Herpetologica*, **6**, 125–135.
- HOCH, D. H., GRODZINSKY, A. J., KOOB, T. J., ALBERT, M. L. & EYRE, D. R. (1983). Early changes in material properties of rabbit articular cartilage after meniscectomy. *Journal of Orthopaedic Research*, **1**, 4–12.
- HOFSTADLER-DEIQUES, C., WALTER, M., MIERLO, F. & RUDUIT, R. (2005). Software system for three-dimensional volumetric reconstruction of histological sections: A case study for the snake chondrocranium. *Anatomical Record*, **286**, 938–944.
- HOWARD, L. E., HOLMES, W. M., FERRANDO, S., MACLAINE, J. S., KELSH, R. N., RAMSEY, A., ABEL, R. L. & COX, J. P. (2013). Functional nasal morphology of chimaerid fishes. *Journal of Morphology*, **274**, 987–1009.
- HOWES, G. B. & SWINNERTON, H. H. (1901). On the development of the skeleton of the tuatara, *Sphenodon punctatus*; with remarks on the egg, on the hatching, and on the hatched young. *The Transactions of the Zoological Society of London*, **16**, 1–84.
- HU, K., QIGUO, R., FANG, J. & MAO, J. J. (2003). Effects of condylar fibrocartilage on the biomechanical loading of the human temporomandibular joint in a three-dimensional, nonlinear finite element model. *Medical Engineering & Physics*, **25**, 107–113.
- HUANG, H., LUO, X., CHENG, X., ZHANG, Z., MA, G., SHI, B. & LI, J. (2018). Recapitulation of unilateral cleft lip nasal deformity on normal nasal structure: a finite element model analysis. *Journal of Craniofacial Surgery*, **29**, 2220–2225.
- HUBER, D. R., EASON, T. G., HUETER, R. E. & MOTTA, P. J. (2005). Analysis of the bite force and mechanical design of the feeding mechanism of the durophagous horn shark *Heterodontus francisci*. *Journal of Experimental Biology*, **208**, 3553–3571.
- HUGI, J., MITGUTSCH, C. & SÁNCHEZ-VILLAGRA, M. R. (2010). Chondrogenic and ossification patterns and sequences in White's skink *Liopholis whitii* (Scincidae, Reptilia). *Zoosystematics and Evolution*, **86**, 21–32.
- HUKINS, D. W. L. & ASPDEN, R. M. (1985). Composition and properties of connective tissues. *Trends in Biochemical Sciences*, **10**, 260–264.
- HÜPPI, E., SÁNCHEZ-VILLAGRA, M. R., TZIKA, A. C. & WERNEBURG, I. (2018). Ontogeny and phylogeny of the mammalian chondrocranium: the cupula nasi anterior and associated structures of the anterior head region. *Zoological Letters*, **4**, 1–29.
- HÜPPI, E., NÚÑEZ-LEÓN, D., NAGASHIMA, H. & SÁNCHEZ-VILLAGRA, M. R. (2019). Development of the chondrocranium in the domesticated fowl (*Gallus gallus f. domestica*), with a study on the variation of the of hypoglossal foramina. *Vertebrate Zoology*, **69**, 299–310.
- JANVIER, P. (2008). Early jawless vertebrates and cyclostome origins. *Zoological Science*, **25**, 1045–1056.
- JEFFREY, J. E. & ASPDEN, R. M. (2006). The biophysical effects of a single impact load on human and bovine articular cartilage. *Proceedings of the Institution of Mechanical Engineers H*, **220**, 677–686.
- JIN, H. & LEWIS, J. L. (2004). Determination of Poisson's ratio of articular cartilage by indentation using different-sized indenters. *Journal of Biomechanical Engineering*, **126**(2), 138–145.
- JONES, M. E. H., BUTTON, D. J., BARRETT, P. M. & PORRO, L. B. (2019). Digital dissection of the head of the rock dove (*Columba livia*) using contrast-enhanced computed tomography. *Zoological Letters*, **5**, 1–32.
- JONES, M. E. H., O'HIGGINS, P., FAGAN, M. J., EVANS, S. E. & CURTIS, N. (2012). Shearing mechanics and the influence of a flexible symphysis during oral food processing in *Sphenodon* (Lepidosauria: Rhynchocephalia). *Anatomical Record*, **295**, 1075–1091.
- JONES, M. E. H., GRÖNING, F., DUTEL, H., SHARP, A., FAGAN, M. J. & EVANS, S. E. (2017). The biomechanical role of the chondrocranium and sutures in a lizard cranium. *Journal of the Royal Society Interface*, **14**, 20170637.
- JONES, M. E. H., PISTEVOS, J. C., COOPER, N., LAPPIN, A. K., GEORGES, A., HUTCHINSON, M. N. & HOLLELEY, C. E. (2020). Reproductive phenotype predicts adult bite-force performance in sex-reversed dragons (*Pogona vitticeps*). *Journal of Experimental Zoology A*, **333**, 252–263.
- KACZMAREK, P., JANISZEWSKA, K., METSCHER, B. & RUPIK, W. (2020). Development of the squamate naso-palatal complex: detailed 3D analysis of the vomeronasal organ and nasal cavity in the brown anole *Anolis sagrei* (Squamata: Iguania). *Frontiers in Zoology*, **17**, 28.
- KAMAL, A. M. & ABDEEN, A. M. (1972). The development of the chondrocranium of the lacertid lizard, *Acanthodactylus boskiana*. *Journal of Morphology*, **137**, 289–333.
- KAUCKA, M., PETERSEN, J., TESAROVA, M., SZAROWSKA, B., KASTRITI, M. E., XIE, M., KICHEVA, A., ANNUSVER, K., KASPER, M., SYMMONS, O. & PAN, L. (2018). Signals from the brain and olfactory epithelium control shaping of the mammalian nasal capsule cartilage. *Elife*, **7**, e34465.
- KAUCKA, M. & ADAMEYKO, I. (2019). Evolution and development of the cartilaginous skull: from a lancelet towards a human face. *Seminars in Cell & Developmental Biology*, **91**, 2–12.
- KEMBLE, J. V. H. (1973). Underdevelopment of the maxilla related to absence of the cartilaginous nasal septum. *British Journal of Plastic Surgery*, **26**, 266–270.
- KLENNER, S., WITZEL, U., PARIS, F. & DISTLER, C. (2016). Structure and function of the septum nasi and the underlying tension chord in crocodylians. *Journal of Anatomy*, **228**, 113–124.
- KLINGER-STROBEL, M., OLSSON, L., GLAW, F. & MÜLLER, H. (2020). Development of the skeleton in the dwarf clawed frog *Pseudohemichirus merlini* (Amphibia: Anura: Pipidae). *Vertebrate Zoology*, **70**, 435–446.
- KRINGS, M., MÜLLER, H., HENEKA, M. J. & RÖDDER, D. (2017a). Modern morphological methods for tadpole studies. A comparison of micro-CT, and clearing and staining protocols modified for frog larvae. *Biotechnic & Histochemistry*, **92**, 595–605.
- KRINGS, M., KLEIN, B., HENEKA, M. J. & RÖDDER, D. (2017b). Morphological comparison of five species of poison dart frogs of the genus *Ranitomeya* (Anura: Dendrobatidae) including the skeleton, the muscle system and inner organs. *PLoS ONE*, **12**, e0171669.
- KUBICEK, K. & CONWAY, K. W. (2015). Developmental osteology of *Sciaenops ocellatus* and *Cynoscion nebulosus* (Teleostei: Sciaenidae), economically important sciaenids from the western Atlantic. *Acta Zoologica*, **97**, 267–301.
- KUPCZIK, K., DOBSON, C. A., FAGAN, M. J., CROMPTON, R. H., OXNARD, C. E. & O'HIGGINS, P. (2007). Assessing mechanical function of the zygomatic region in macaques: validation and sensitivity testing of finite element models. *Journal of Anatomy*, **210**, 41–53.
- KURATANI, S. (1999). Development of the chondrocranium of the loggerhead turtle, *Caretta caretta*. *Zoological Science*, **16**, 803–818.
- KURATANI, S. & AHLBERG, P. E. (2018). Evolution of the vertebrate neurocranium: problems of the premandibular domain and the origin of the trabecula. *Zoological Letters*, **4**, 1–10.
- LAKING, B. A., SNYDER, B. D. & GRINSTAFF, M. W. (2017). Assessing cartilage biomechanical properties: techniques for evaluating



- the functional performance of cartilage in health and disease. *Annual Review of Biomedical Engineering*, **19**, 27–55.
- LANGELIER, E. & BUSCHMANN, M. D. (2003). Increasing strain and strain rate strengthen transient stiffness but weaken the response to subsequent compression for articular cartilage in unconfined compression. *Journal of Biomechanics*, **36**, 853–859.
- LAPPIN, A. K. & JONES, M. E. H. (2014). Reliable quantification of bite-force performance requires use of appropriate biting substrate and standardization of bite out-lever. *Journal of Experimental Biology*, **217**, 4303–4312.
- LAPPIN, A. K., WILCOX, S. C., MORIARTY, D. J., STOEPPLER, S. A., EVANS, S. E. & JONES, M. E. H. (2017). Bite force in the horned frog (*Ceratophrys cranwelli*) with implications for extinct giant frogs. *Scientific Reports*, **7**, 11963.
- LAVERNA, L., BROWN, W. E., WONG, B. J., HU, J. C. & ATHANASIOU, K. A. (2019). Toward tissue-engineering of nasal cartilages. *Acta Biomaterialia*, **88**, 42–56.
- LARSON, P. M. & DE SÁ, R. O. (1998). Chondrocranial morphology of *Leptodactylus* larvae (Leptodactylidae: Leptodactylinae): its utility in phylogenetic reconstruction. *Journal of Morphology*, **238**, 287–305.
- LEARY, R. P., MANUEL, C. T., SHAMOUELIAN, D., PROTSENKO, D. E. & WONG, B. J. (2015). Finite element model analysis of cephalic trim on nasal tip stability. *Journal of the American Medical Association Facial Plastic Surgery*, **17**, 413–420.
- LEE, S. J., LIONG, K. & LEE, H. P. (2010). Deformation of nasal septum during nasal trauma. *Laryngoscope*, **120**, 1931–1939.
- LIBBY, J., MARGHOUB, A., JOHNSON, D., KHONSARI, R. H., FAGAN, M. J. & MOAZEN, M. (2017). Modelling human skull growth: a validated computational model. *Journal of the Royal Society Interface*, **14**, 20170202.
- LIPPHAUS, A. & WITZEL, U. (2020). Three-dimensional finite element analysis of the dural folds and the human skull under head acceleration. *Anatomical Record*. doi: 10.1002/ar.24401.
- LITTLE, C. J., BAWOLIN, N. K. & CHEN, X. (2011). Mechanical properties of natural cartilage and tissue-engineered constructs. *Tissue Engineering Part B: Reviews*, **17**, 213–227.
- LIU, X., DEAN, M. N., YOUSSEFFOUR, H., SUMMERS, A. P. & EARTHMAN, J. C. (2014). Stress relaxation behavior of tessellated cartilage from the jaws of blue sharks. *Journal of the Mechanical Behavior of Biomedical Materials*, **29**, 68–80.
- LOEB, G. E., LOEB, G. & GANS, C. (1986). *Electromyography for Experimentalists*. Chicago, IL, University of Chicago Press.
- LONG, J. A., BURROW, C. J., GINTER, M., MAISEY, J. G., TRINAUSTIC, K. M., COATES, M. I., YOUNG, G. C. & SENDEN, T. J. (2015). First shark from the Late Devonian (Frasnian) Gogo Formation, Western Australia sheds new light on the development of tessellated calcified cartilage. *PLoS ONE*, **10**, e0126066.
- LOZANOFF, S., ZINGESER, M. R. & DIEWERT, V. M. (1993). Computerized modelling of nasal capsular morphogenesis in prenatal primates. *Clinical Anatomy*, **6**, 37–47.
- LU, J., ZHU, M., LONG, J. A., ZHAO, W., SENDEN, T. J., JIA, L. & QIAO, T. (2012). The earliest known stem-tetrapod from the Lower Devonian of China. *Nature Communications*, **3**, 1–7.
- LU, J., ZHU, M., AHLBERG, P. E., QIAO, T., ZHU, Y. A., ZHAO, W. & JIA, L. (2016). A Devonian predatory fish provides insights into the early evolution of modern sarcopterygians. *Science Advances*, **2**, e1600154.
- MAIER, W. (2020). A neglected part of the mammalian skull: The outer nasal cartilages as progressive remnants of the chondrocranium. *Vertebrate Zoology*, **70**, 367–382.
- MAISEY, J. G. (2013). The diversity of tessellated calcification in modern and extinct chondrichthyans. *Revue de Paléobiologie*, **32**, 355–371.
- MANSOUR, J. M. (2004). Biomechanics of Cartilage, pp. 68–79 in: OATIS, C. A. (ed.), *Kinesiology: The Mechanics and Pathomechanics of Human Movement*. Philadelphia, PA, Lippincott Williams & Wilkins.
- MANUEL, C. T., LEARY, R., PROTSENKO, D. E. & WONG, B. J. (2014). Nasal tip support: A finite element analysis of the role of the caudal septum during tip depression. *Laryngoscope*, **124**, 649–654.
- MARÇÉ-NOGUÉ, J., KŁODOWSKI, A., SÁNCHEZ, M. & GIL, L. (2015). Coupling finite element analysis and multibody system dynamics for biological research. *Palaeontologia Electronica*, **18**, 1–14.
- MARA, K. R., MOTTA, P. J., MARTIN, A. P. & HUETER, R. E. (2015). Constructional morphology within the head of hammerhead sharks (Sphyrnidae). *Journal of Morphology*, **276**, 526–539.
- MARKEY, M. J., MAIN, R. P. & MARSHALL, C. R. (2006). *In vivo* cranial suture function and suture morphology in the extant fish *Polypterus*: implications for inferring skull function in living and fossil fish. *Journal of Experimental Biology*, **209**, 2085–2102.
- MATTOX, G. M., BRITZ, R. & TOLEDO-PIZA, M. (2014). Skeletal development and ossification sequence of the characiform *Salmimus brasiliensis* (Ostariophysi: Characidae). *Ichthyological Exploration of Freshwaters*, **25**, 103–158.
- MCBRATNEY-OWEN, B., ISEKI, S., BAMFORTH, S. D., OLSEN, B. R. & MORRIS-KAY, G. M. (2008). Development and tissue origins of the mammalian cranial base. *Developmental Biology*, **322**, 121–132.
- MCCORMACK, S. W., WITZEL, U., WATSON, P. J., FAGAN, M. J. & GRÖNING, F. (2017). Inclusion of periodontal ligament fibres in mandibular finite element models leads to an increase in alveolar bone strains. *PLoS ONE*, **12**, e0188707.
- MCQUISTON, A. D., CRAWFORD, C., SCHOEPE, U. J., VARGA-SZEMES, A., CANSTEIN, C., RENKER, M., DE CECCO, C. N., BAUMANN, S. & NAYLOR, G. J. (2017). Segmentations of the cartilaginous skeletons of chondrichthyan fishes by the use of state-of-the-art computed tomography. *World Journal of Radiology*, **9**, 191–198.
- MCHENRY, C. R., WROE, S., CLAUSEN, P. D., MORENO, K. & CUNNINGHAM, E. (2007). Supermodeled sabercat, predatory behavior in *Smilodon fatalis* revealed by high-resolution 3D computer simulation. *Proceedings of the National Academy of Sciences*, **104**, 16010–16015.
- MEISAMI, E. & BHATNAGAR, K. P. (1998). Structure and diversity in mammalian accessory olfactory bulb. *Microscopy Research and Technique*, **43**, 476–499.
- METSCHER, B. D. (2009). MicroCT for comparative morphology: Simple staining methods allow high-contrast 3D imaging of diverse non-mineralized animal tissues. *BMC Physiology*, **9**, 1–14.
- MEAD, C. S. (1909). The chondrocranium of an embryo pig, *Sus scrofa*. A contribution to the morphology of the mammalian skull. *American Journal of Anatomy*, **9**, 167–209.
- MENAPACE, D. C., CARLSON, K. D., DRAGOMIR-DAESCU, D., MATSUMOTO, J. & HAMILTON, G. S. (2020). Finite element analysis of the septal cartilage L-strut. *Facial Plastic Surgery & Aesthetic Medicine*. doi: 10.1089/fpsam.2019.0012.
- MEZZASALMA, M., MAIO, N. & GUARINO, F. M. (2014). To move or not to move: Cranial joints in European gekkotans and laceratids, an osteological and histological perspective. *Anatomical Record*, **297**, 463–472.
- MIKALSEN, Å. K. R., FOLSTAD, I., YOCOZ, N. G. & LAENG, B. (2014). The spectacular human nose: an amplifier of individual quality? *PeerJ*, **2**, e357.
- MIIYAKE, T., MCEACHRAN, J. D., WALTON, P. J. & HALL, B. K. (1992). Development and morphology of rostral cartilages in batoid fishes (Chondrichthyes: Batoidea), with comments on homology within vertebrates. *Biological Journal of the Linnean Society*, **46**, 259–298.
- MOAZEN, M., CURTIS, N., EVANS, S. E., O'HIGGINS, P. & FAGAN, M. J. (2008). Combined finite element and multibody dynamics analysis of biting in a *Uromastyx hardwickii* lizard skull. *Journal of Anatomy*, **213**, 499–508.
- MOAZEN, M., CURTIS, N., O'HIGGINS, P., JONES, M. E. H., EVANS, S. E. & FAGAN, M. J. (2009). Assessment of the role of sutures in a lizard skull: a computer modelling study. *Proceedings of the Royal Society B*, **276**, 39–46.

- MOSS, M. L., BROMBERG, B. E., SONG, I. G. & EISENMAN, G. (1968). The passive role of nasal septal cartilage in mid-facial growth. *Plastic and Reconstructive Surgery*, **41**, 536–542.
- NIKLAS, K. J. (1992). *Plant Biomechanics: An Engineering Approach to Plant Form and Function*. Chicago, IL, University of Chicago Press.
- NORMAN, J. R. (1926). The development of the chondrocranium of the eel (*Anguilla vulgaris*), with observations on the comparative morphology and development of the chondrocranium in bony fishes. *Philosophical Transactions of the Royal Society of London B*, **214**, 369–464.
- OISI, Y., OTA, K. G., FUJIMOTO, S. & KURATANI, S. (2013). Development of the chondrocranium in hagfishes, with special reference to the early evolution of vertebrates. *Zoological Science*, **30**, 944–961.
- PALUH D. J. & SHEIL, C. A. (2013). Anatomy of the fully formed chondrocranium of *Emydura subglobosa* (Chelidae): A pleurodiran turtle. *Journal of Morphology*, **274**, 1–10.
- PAPHANGKORAKIT, J. & OSBORN, J. W. (1998). Effects on human maximum bite force of biting on a softer or harder object. *Archives of Oral Biology*, **43**, 833–839.
- PARDO, J. D., HUTTENLOCKER, A. K. & SMALL, B. J. (2014). An exceptionally preserved transitional lungfish from the Lower Permian of Nebraska, USA, and the origin of modern lungfishes. *PLoS ONE*, **9**, e108542.
- PARKER, W. K. (1883). On the structure and development of the skull in the Crocodylia. *Transactions of the Zoological Society of London*, **11**, 263–310.
- PATTERSON, C. (1975). The braincase of pholidophorid and leptolepid fishes, with a review of the actinopterygian braincase. *Philosophical Transactions of the Royal Society of London B*, **269**, 275–579.
- PAYNE, S. L., HOLLIDAY, C. M. & VICKARYOUS, M. K. (2011). An osteological and histological investigation of cranial joints in geckos. *Anatomical Record*, **294**, 399–405.
- PEARSON, H. S. (1921). The skull and some related structures of a late embryo of *Lygosoma*. *Journal of Anatomy*, **56**, 20–43.
- PETERS, A. E., COMERFORD, E. J., MACAULAY, S., BATES, K. T. & AKHTAR, R. (2017). Micromechanical properties of canine femoral articular cartilage following multiple freeze-thaw cycles. *Journal of the Mechanical Behavior of Biomedical Materials*, **71**, 114–121.
- PORRO, L. B., METZGER, K. A., IRIARTE-DIAZ, J. & ROSS, C. F. (2013). *In vivo* bone strain and finite element modeling of the mandible of *Alligator mississippiensis*. *Journal of Anatomy*, **223**, 195–227.
- PORRO, L. B., ROSS, C. F., IRIARTE-DIAZ, J., O'REILLY, J. C., EVANS, S. E. & FAGAN, M. J. (2014). *In vivo* cranial bone strain and bite force in the agamid lizard *Uromastyx geyri*. *Journal of Experimental Biology*, **217**, 1983–1992.
- PORTER, M. E., BELTRAN, J. L., KOOB, T. J. & SUMMER, A. P. (2006). Material properties and biochemical composition of mineralized vertebral cartilage in seven elasmobranch species (Chondrichthyes). *Journal of Experimental Biology*, **209**, 2920–2928.
- PORTER, M. E., BELTRAN, J. L., KAJIURA, S. M., KOOB, T. J. & SUMMERS, A. P. (2013). Stiffness without mineral: Material properties and biochemical components of jaws and chondrocrania in the Elasmobranchii (sharks, skates, and rays). *PeerJ PrePrints*, **1**, e47v1.
- RAFFERTY, K. L., HERRING, S. W. & MARSHALL, C. D. (2003). Biomechanics of the rostrum and the role of facial sutures. *Journal of Morphology*, **257**, 33–44.
- RAYFIELD, E. J. (2007). Finite element analysis and understanding the biomechanics and evolution of living and fossil organisms. *Annual Review of Earth and Planetary Sciences*, **35**, 541–576.
- RICHMOND, J. D., SAGE, A., WONG, V. W., CHEN, A. C., SAH, R. L. & WATSON, D. (2006). Compressive biomechanical properties of human nasal septal cartilage. *American Journal of Rhinology*, **20**, 496–501.
- RICHMOND, B. G., WRIGHT, B. W., GROSSE, I., DECHOW, P. C., ROSS, C. F., SPENCER, M. A. & STRAIT, D. S. (2005). Finite element analysis in functional morphology. *Anatomical Record*, **283**, 259–274.
- REILLY, S. M., MCBRAYER, L. D. & WHITE, T. D. (2001). Prey processing in amniotes: biomechanical and behavioral patterns of food reduction. *Comparative Biochemistry and Physiology A*, **128**, 397–415.
- REMMLER, D., OLSON, L., EKSTROM, R., DUKE, D., MATAMOROS, A., MATTHEWS, D. & ULLRICH, C. G. (1998). Pre-surgical CT/FEA for craniofacial distraction: I.: Methodology, development, and validation of the cranial finite element model. *Medical Engineering & Physics*, **20**, 607–619.
- ROČEK, Z., PŘIKRYL, T., BALEEVA, N., VAZEILLE, A., BOISTEL, R., BRAVIN, A., NEMOZ, C., VAN DIJK, E., SMIRINA, E. M. & CLAESSENS, L. (2016). Contribution to the head anatomy of the basal frog *Barbourula busuangensis* and the evolution of the Anura. *Russian Journal of Herpetology*, **23**, 163–194.
- ROSS, C. F. (2005). Finite element analysis in vertebrate biomechanics. *Anatomical Record*, **283**, 253–258.
- ROSS, C. F. & HYLANDER, W. L. (1996). *In vivo* and *in vitro* bone strain in the owl monkey circumorbital region and the function of the postorbital septum. *American Journal of Physical Anthropology*, **101**, 183–215.
- ROSS, C. F. & METZGER, K. A. (2004). Bone strain gradients and optimization in vertebrate skulls. *Annals of Anatomy Anatomischer Anzeiger*, **186**, 387–396.
- ROSS, C. F., BADEN, A. L., GEORGI, J., HERREL, A., METZGER, K. A., REED, D. A., SCHAERLAEKEN, V. & WOLFF, M. S. (2010). Chewing variation in lepidosaurs and primates. *Journal of Experimental Biology*, **213**, 572–584.
- RYCHEL, A. L. & SWALLA, B. J. (2007). Development and evolution of chordate cartilage. *Journal of Experimental Zoology Part B*, **308**, 325–335.
- SÁNCHEZ-VILLAGRA, M. & FORASIEPI, A. M. (2017). On the development of the chondrocranium and the histological anatomy of the head in perinatal stages of marsupial mammals. *Zoology Letters*, **3**, 1–33.
- SARNAT, B. G. (2008). Some factors related to experimental snout growth. *Journal of Craniofacial Surgery*, **19**, 1308–1314.
- SARNAT, B. G. & WEXLER, M. R. (1966). Growth of the face and jaws after resection of the septal cartilage in the rabbit. *American Journal of Anatomy*, **118**, 755–767.
- SASAZAKI, Y., SHORE, R. & SEEDHOM, B. B. (2006). Deformation and failure of cartilage in the tensile mode. *Journal of Anatomy*, **208**, 681–694.
- SELLERS, K. C., MIDDLETON, K. M., DAVIS, J. L. & HOLLIDAY, C. M. (2017). Ontogeny of bite force in a validated biomechanical model of the American alligator. *Journal of Experimental Biology*, **220**, 2036–2046.
- SHAMOUELIAN, D., LEARY, R. P., MANUEL, C. T., HARB, R., PROTSENKO, D. E. & WONG, B. J. (2015). Rethinking nasal tip support: a finite element analysis. *Laryngoscope*, **125**, 326–330.
- SHEIL, C. A. & ZAHAREWICZ, K. (2014). Anatomy of the fully formed chondrocranium of *Podocnemis unifilis* (Pleurodira: Podocnemididae). *Acta Zoologica*, **95**, 358–366.
- SOKOL, O. M. (1981). The larval chondrocranium of *Pelodytes punctatus*, with a review of tadpole chondrocrania. *Journal of Morphology*, **169**(2), 161–183.
- SQUARE, T. A., JANDZIK, D., MASSEY, J. L., ROMÁŠEK, M., STEIN, H. P., HANSEN, A. W., PURKAYASTHA, A., CATTELL, M. V. & MEDEIROS, D. M. (2020). Evolution of the endothelin pathway drove neural crest cell diversification. *Nature*, **585**, 563–568.
- SMITH, T. D., UFELLE, A., CRAY, J. J., REHOREK, S. B. & DELEON, V. B. (2020). An inward collapse of the nasal cavity: perinatal consolidation of the midface and cranial base in primates. *Anatomical Record*, doi: 10.1002/ar.24537.
- STENSTRÖM, S. J. & THILANDER, B. L. (1970). Effects of nasal septal cartilage resections on young guinea pigs. *Plastic and Reconstructive Surgery*, **45**, 160–170.

- TARAZONA, O. A., SLOTA, L. A., LOPEZ, D. H., ZHANG, G. & COHN, M. J. (2016). The genetic program for cartilage development has deep homology within Bilateria. *Nature*, **533**, 86–89.
- TESAROVÁ, M., ZIKMUND, T., KAUKÁ, M., ADAMEYKO, I. & KAISER, J. (2019). Use of the industrial X-ray computed microtomography to address scientific questions in developmental biology. *NDT.net*, **2019**, 1–9.
- THESKA, T., WILKINSON, M., GOWER, D. J. & MÜLLER, H. (2019). Musculoskeletal development of the central African caecilian *Idiocranium russeli* (Amphibia: Gymnophiona: Indotyphlidae) and its bearing on the re-evolution of larvae in caecilian amphibians. *Zoomorphology*, **138**, 137–158.
- THOMASON, J. J., GROVUM, L. E., DESWYSEN, A. G. & BIGNELL, W. W. (2001). *In vivo* surface strain and stereology of the frontal and maxillary bones of sheep: implications for the structural design of the mammalian skull. *Anatomical Record*, **264**, 325–338.
- TSE, K. M., TAN, L. B., LEE, S. J., LIM, S. P. & LEE, H. P. (2015). Investigation of the relationship between facial injuries and traumatic brain injuries using a realistic subject-specific finite element head model. *Accident Analysis & Prevention*, **79**, 3–32.
- VAN VUUREN, L. J., BROADBENT, J. M., DUNCAN, W. J. & WADDELL, J. N. (2020). Maximum voluntary bite force, occlusal contact points and associated stresses on posterior teeth. *Journal of the Royal Society of New Zealand*, **50**, 132–143.
- WALLER, G. N. H. & BARANES, A. (1991). Chondrocranium morphology of northern red sea triakid sharks and relationships to feeding habits. *Journal of Fish Biology*, **38**, 715–730.
- WARTH, P., HILTON, E. J., NAUMANN, B., OLSSON, L. & KONSTANTINIDIS, P. (2017). Development of the skull and pectoral girdle in Siberian sturgeon, *Acipenser baerii*, and Russian sturgeon, *Acipenser gueldenstaedtii* (Acipenseriformes: Acipenseridae). *Journal of Morphology*, **278**, 418–442.
- WERNEBURG, I. & YARYHIN, O. (2019). Character definition and tempus optimum in comparative chondrocranial research. *Acta Zoologica*, **100**, 376–388.
- WESTREICH, R. W., COURTLAND, H. W., NASSER, P., JEPSEN, K. & LAWSON, W. (2007). Defining nasal cartilage elasticity: biomechanical testing of the tripod theory based on a cantilevered model. *Archives of Facial Plastic Surgery*, **9**, 264–270.
- WEXLER, M. R. & SARNAT, B. G. (1965). Rabbit snout growth after dislocation of nasal septum. *Archives of Otolaryngology*, **81**, 68–71.
- WILKEN, A. T., SELLERS, K. C., COST, I. N., ROZIN, R. E., MIDDLETON, K. M. & HOLLIDAY, C. M. (2020). Connecting the chondrocranium: Biomechanics of the suspensorium in reptiles. *Vertebrate Zoology*, **70**, 275–290.
- WITMER, L. M. (1995). Homology of facial structures in extant archosaurs (birds and crocodylians), with special reference to paranasal pneumaticity and nasal conchae. *Journal of Morphology*, **225**, 269–327.
- WITTEN, P. E., HUYSSSEUNE, A. & HALL, B. K. (2010). A practical approach for the identification of the many cartilaginous tissues in teleost fish. *Journal of Applied Ichthyology*, **26**, 257–262.
- WOOD, A., ASHHURST, D. E., CORBETT, A. & THOROGOOD, P. (1991). The transient expression of type II collagen at tissue interfaces during mammalian craniofacial development. *Development*, **111**, 955–968.
- WROE, S., HUBER, D. R., LOWRY, M., MCHENRY, C., MORENO, K., CLAUSEN, P., FERRARA, T. L., CUNNINGHAM, E., DEAN, M. N. & SUMMERS, A. P. (2008). Three-dimensional computer analysis of white shark jaw mechanics: how hard can a Great White bite? *Journal of Zoology*, **276**, 336–342.
- WROE, S., PARR, W. C., LEDOGAR, J. A., BOURKE, J., EVANS, S. P., FIORENZA, L., BENAZZI, S., HUBLIN, J. J., STRINGER, C., KULLMER, O. & CURRY, M. (2018). Computer simulations show that Neanderthal facial morphology represents adaptation to cold and high energy demands, but not heavy biting. *Proceedings of the Royal Society B*, **285**, 20180085.
- WRIGHT, V. & DOWSON, D. (1976). Lubrication and cartilage. *Journal of Anatomy*, **121**, 107–118.
- XIA, Y., ZHENG, S., SZARKO, M. & LEE, J. (2012). Anisotropic properties of bovine nasal cartilage. *Microscopy Research and Technique*, **75**, 300–306.
- YARYHIN, O. & WERNEBURG, I. (2018). Tracing the developmental origin of a lizard skull: chondrocranial architecture, heterochrony, and variation in lacertids. *Journal of Morphology*, **279**, 1058–1087.
- YARYHIN, O. & WERNEBURG, I. (2019). The origin of orbitotemporal diversity in lepidosaurs: insights from tuatara chondrocranial anatomy. *Vertebrate Zoology*, **69**, 169–181.
- ZADA, S. (1981). The fully formed chondrocranium of the agamid lizard, *Agama pallida*. *Journal of Morphology*, **170**, 43–54.
- ZAHER, M. M. & ABU-TAIRA, A. M. (2013). A review on the avian chondrocranium. *The Journal of Basic & Applied Zoology*, **66**, 109–120.
- ZAIDI, A. A., MATTERN, B. C., CLAES, P., MCEVOY, B., HUGHES, C. & SHRIVER, M. D. (2018). Correction: Investigating the case of human nose shape and climate adaptation. *PLoS Genetics*, **13**, e1006616.
- ZAHNERT, T., HÜTTENBRINK, K. B., MÜRBE, D. & BORNITZ, M. (2000). Experimental investigations of the use of cartilage in tympanic membrane reconstruction. *Otology & Neurotology*, **21**, 322–328.
- ZHANG, L., YANG, K. H. & KING, A. I. (2001). Comparison of brain responses between frontal and lateral impacts by finite element modeling. *Journal of Neurotrauma*, **18**, 21–30.
- ZHANG, G., MIYAMOTO, M. M. & COHN, M. J. (2006). Lamprey type II collagen and Sox9 reveal an ancient origin of the vertebrate collagenous skeleton. *Proceedings of the National Academy of Sciences*, **103**, 3180–3185.
- ZHENG, H., PERRINE, S. M. M., PITIRRI, M. K., KAWASAKI, K., WANG, C., RICHTSMIEIER, J. T. & CHEN, D. Z. (2020). Cartilage segmentation in high-resolution 3D micro-CT images via uncertainty-guided self-training with very sparse annotation, pp. 802–812 in: MARTEL A. L., ABOLMAESUMI, P., STOYANOV, D., MATEUS, D., ZULUAGA, M. A., ZHOU, S. K., RACOCEANU, D. & JOSKOWICZ, L. (eds) *Medical Image Computing and Computer Assisted Intervention – MICCAI 2020. Lecture Notes in Computer Science, Vol. 12261*. Cham, Springer.
- ZHU, M. (2014). Bone gain and loss: Insights from genomes and fossils. *National Science Review*, **1**, 490–492.
- ZHU, M., YU, X., AHLBERG, P. E., CHOO, B., LU, J., QIAO, T., QU, Q., ZHAO, W., JIA, L., BLOM, H. & ZHU, Y. A. (2013). A Silurian placoderm with osteichthyan-like marginal jaw bones. *Nature*, **502**, 188–193.
- ZHU, Z., ZHANG, W. & WU, C. (2014). Energy conversion in woodpecker on successive peckings and its role on anti-shock protection of brain. *Science China Technological Sciences*, **57**, 1269–1275.

